Ministry of higher education and scientific research

وزارة التـعليـم العالـي والبحـث العلمــي

University of Ain Temouchent, Belhadj Bouchaib

جامعة بلحاج بوشعيب لعين تموشنت

Faculty of Sciences and Technology

Department of Materials Science

Field: Science of matter

Specialty: Materials Physics

SECOND YEAR M2 –PHYSICS

Course Name:

Functional Materials and Nanostructures

Presented By:

Dr. TOUIA Amina

Academic year 2022/2023

بسم الله الرحمن الرحيم

Preface

This document was intended for second-year Master's students in physics at the University of Ain Temouchent, Belhadj Bouchaib. It responds to the official program of the "Functional Materials and Nanostructures" module taught in the second year of the master's degree in materials physics. It was written in the form of a detailed course, consisting of four chapters.

Specified objectives:

- Gain insight into functional materials that are important for applications.
- A deep understanding of the physical concepts and mechanisms of thermoelectric, piezoelectric, magnetostrictive, and nanostructured materials.

TABLE OF CONTENTS

TABLE OF CONTENTS

CHAPTER I

THERMOELECTRIC MATERIALS

CHAPTER I: THERMOELECTRIC MATERIALS

I.   Introduction:

   This introductory chapter chronologically describes the various discoveries made regarding this theme. Research on thermoelectricity, an effect linking the flow of heat that crosses a material to the electric current that runs through it, which will lead us to present different applications, current and future, exploiting thermoelectric conversion systems, production of electric current from a source of heat, and vice-versa, is currently undergoing significant development linked to research on new sources of non-polluting energy for the future, environmental problems, and access to energy ,which are among the major challenges of the 21st century. At the end of this chapter, various thermoelectric compounds currently being studied for thermoelectric applications are presented.

I.1. History of thermoelectric materials:

   Volta was the first in **1794** to demonstrate a thermoelectric phenomenon. Mario Glozzi's book "Storia della Fisica" of **1796**, includes a section "thermoelectric effect" he indicates that Volta had put one end of an iron conductor in boiling water and observed the effect of a current electric on a frog. Therefore, this is a thermoelectric phenomenon. But it was not until **1821** that Thomas Johann Seebeck, a German physicist, highlighted the potential difference that is created at the junction between two materials when they are subjected to a temperature gradient (Seebeck coefficient S = $\Delta V/\Delta T$) **[1]**. Composed of a simple ring of half-bismuth and half-copper, his experiment showed that by heating the junction between the two metals, a current appeared and circulated in the ring, capable of deflecting a magnetic needle **[1]**. Although he falsely attributed this result to the appearance of a magnetic field, he had just invented a thermoelectric battery using a new effect that would later be called: the Seebeck effect. In **1834**, a French watchmaker and inventor based in Geneva, Jean Peltier, discovered a second thermoelectric effect: a difference in temperature appears at the junctions of two materials of different natures that are subjected to an electric current. In **1838**, a Baltic German physicist, Heinrich Lenz, showed that heat is

CHAPTER I: THERMOELECTRIC MATERIALS

absorbed or released at a thermoelectric junction depending on the direction of the current. In **1851**, English physicist, William Thomson (Lord Kelvin) showed that Seebeck and Peltier effects are linked **[2]**; a material subjected to a thermal gradient and traversed by an electric current exchanges heat with the external environment. Conversely, an electric current is generated by a material subjected to a thermal gradient and traversed by heat flow. The fundamental difference between the Seebeck and Peltier effects is considered separately, and the Thomson effect refers to the existence of the latter for a single material and the uselessness of a junction.

In **1909**, a German thermodynamics, Edmund Altenkirch, correctly calculated for the first time the energy efficiency of a thermoelectric generator based on the Seebeck effect for the first time. In **1949**, a Russian academician and researcher, A.F. IOFFE, developed a theory on thermoelectric semiconductors **[3]**. In **1956**, the same author conceived the idea of alloying, or forming solid solutions and, isomorphic semiconductors with to reduce the thermal conductivity of thermoelectric materials **[4]**. Owing to the lack of progress until the **1970**, it was postulated that a ZT of 1 was a thermoelectric efficiency barrier. This empirical limit has greatly altered the interest in research in the field of thermoelectricity, as a ZT of at least 3 is necessary to compete with conventional refrigeration systems using heat transfer fluids. In the early **1990**, hope was reborn with the theoretical work of Hicks and Dresselhaus **[5,6]**, who proposed the use of materials with low-dimensional structures. According to their calculations, the use of bismuth tellurium (Bi_2Te_3) with a multi-quantum well-type structure enables the multiplication of the factor of merit of massive Bi_2Te_3 by 13 **[5]**. Similarly, a spectacular ZT of 1.4 is predicted for quantum wires based on Bi_2Te_3 **[6]**. Such predictions at the very time when nanotechnology is exploding have therefore caused renewed interest in research on thermoelectricity. However, it was not until the early **2000** that the first nanostructured thermoelectric materials appeared, With ZT exceeding the empirical limit of 1. Venkatasubramanian et al. **[7]** put forward in **2001** superlattices made up of thin layers of Bi_2Te_3 and antimony tellurium (Sb_2Te_3) with a record ZT of 2.4 at room temperature. The following year, Harman et al. presented

CHAPTER I: THERMOELECTRIC MATERIALS

PbSeTe-based quantum dot super lattices with a ZT of 1.6 at room temperature [8]. Hsu et al. **2004** proposed a bulk material based on $AgPb_mSbTe_{2+m}$ comprising nanometric inclusions rich in Ag-Sb with a ZT of ~2.2 at a temperature of 800K [9]. Although this temperature is too high for Although this temperature is too high to consider applications in refrigeration, this type of material can still be interesting for the generation of electrical energy.

In **2008**, Poudel et al proposed to carry out the mechano-synthesis of massive BiSbTe alloys composed of a multitude of nanometric grains. The materials obtained then have a maximum ZT of 1.4 at a temperature of 100°C [10]. In the same year, two studies revealed a ZT of 0.6 at 300 K and 1 at 200 K for silicon nanowires, while the ZT for bulk silicon is approximately 0.01 at 300 K [11].

Currently, research in this field focuses on optimizing the merit factor, which has taken on its full scope since the early **2000** with the rapid development of nanotechnologies and, more particularly, nano-fabrication techniques. Nanostructuring effectively makes it possible to modulate the properties of materials independently and, therefore brings a renewal in the field of thermoelectric research [12].

I.2. Contemporary situation and renaissance:

Since **1960**, scientific research in the field of thermoelectricity has become insignificant, and no school in the world has taught this discipline any longer, whereas at the INPI, only a few very rare patent applications have been filed.

The first oil shock of **1973** did not alter this situation. However, in the united states, NASA still had for the space field, whereas in France, three small entities still dealt with thermoelectricity.

In **1996**, a new fact occurred: the INPI suddenly recorded very strong applications for patents for inventions in the field of thermoelectricity. The number of requests continued to increase from year to year, and in **2005**, this increase became almost exponential.

CHAPTER I: THERMOELECTRIC MATERIALS

Half a century after Abram Ioffé, several hundred patent applications for thermoelectrecity were registered at the INPI each year, whereas before **1996**, applications were reduced to one or two units per year and most often, to none!

Currently, thermoelectricity is being taught again, including in prestigious schools world-wide. Currently, there is no proven explanation for this renewed interest, but we know that this renaissance has come to a good start in France if we look at the number of patents filed and the number of completed university theses.

I.3. Thermoelectric materials:

I.3.1. Materials used in current systems:

This section presents the main thermoelectric materials based on their application temperature ranges. Thermoelectric materials exhibit good thermoelectric performance only in a restricted temperature range, where their reduced figure of merit reaches a maximum and remains approximately constant. Thus, the average application temperature dictates the choice of the thermoelectric material **[13]**. Therefore, thermoelectric materials should be considered based on their temperature ranges. Graphs, such as those of C. Godart in **2009 [14]**, list the evolution of ZT as a function of the temperature of the main n-type (Figure I.1) and p-type (Figure I.2) thermoelectric materials.

The figure of merit (ZT) is given by the following relationship: $ZT = \sigma S^2 T / \kappa$ where S is the Seebeck coefficient, σ is the electrical conductivity, T is the temperature and κ is the thermal conductivity.
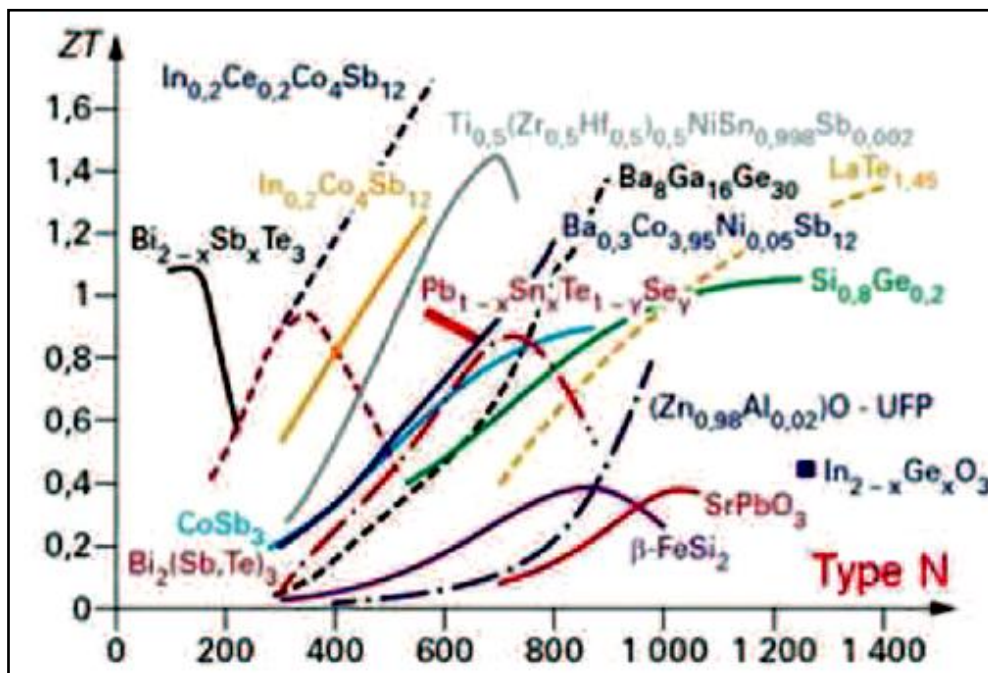
Figure I.1: Figure of merit of n-type thermoelectric materials as a function of temperature **[14]**.

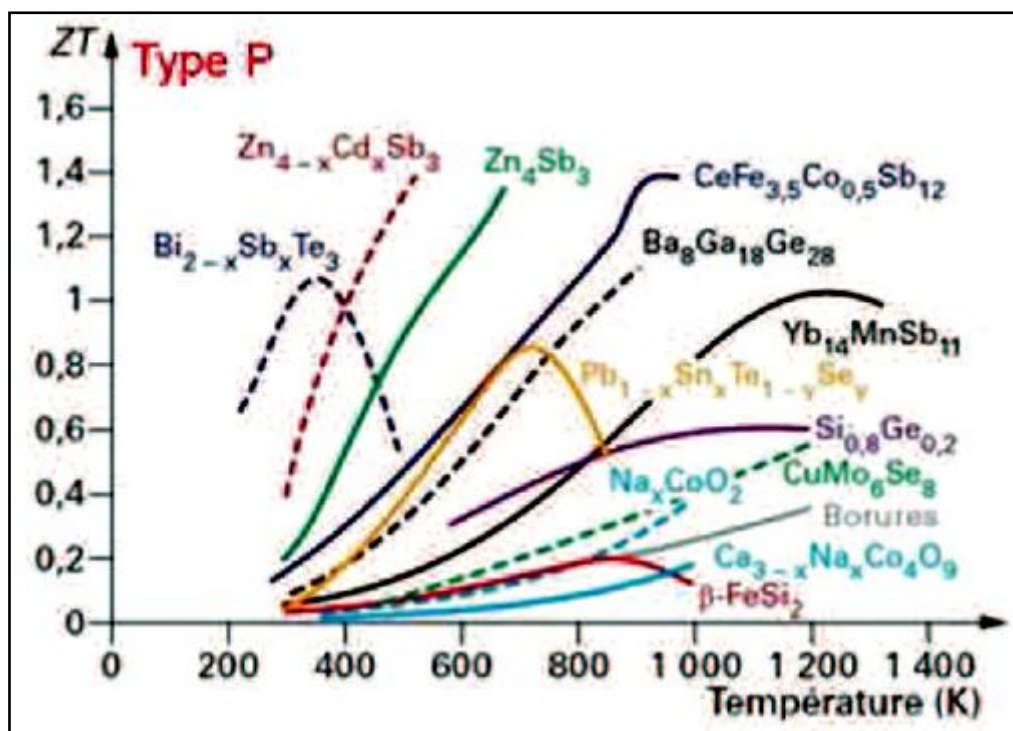Thermoelectric materials that perform well in different temperature ranges are detailed below.

Figure I.2: Figure of merit of P-type thermoelectric materials as a function of temperature **[14]**.

CHAPTER I: THERMOELECTRIC MATERIALS

A. Low temperatures:

The most frequently used thermoelectric material at low temperatures (150 K-200 K), is made on the basis of $Bi_{1-x}Sb_x$ (alloy of bismuth and antimony) and unfortunately only has good thermoelectric properties in n-type (conduction by electrons), which restricts the conversion efficiency of the device since no material is effective in p-type in this temperature range (remember that a thermoelectric conversion device is made up of both p and n branches). Curiously, while its properties are quite average (ZT~0.6), the application of a magnetic field doubles the figure of merit, which then exceeds unity. This material is most often used in combination with permanent magnets [15].

B. Near ambient temperature:

The most studied material is Bi_2Te_3 (an alloy of bismuth and tellurium). It is used in all systems operating near ambient temperature, including the majority of thermoelectric refrigeration systems. The best performance is obtained when it is alloyed with Sb_2Te_3 (alloy of antimony and tellurium), which has the same crystalline structure [16]. Both p-type and n-type samples can be obtained by small compositional variations near stoichiometry. In both cases, ZT values close to 1 were obtained near the ambient temperature [17]. These good ZT values were partly obtained owing to the very low thermal conductivity λ, which is close to 1 $W.m^1.K^{-1}$ for the best materials.

C. Intermediate temperatures:

For use at medium temperatures (550 K -750 K approximately), the most commonly used materials are PbTe and its alloys (PbSn) Te (Sn = tin). The two compounds PbTe and SnTe can form a complete solid solution, which makes it possible to optimize the gap (band gap of the semiconductor) to the desired value. The best materials obtained have merit factors close to unity at approximately 700 K [18]. However, these values were obtained only for the n-type materials. Therefore, at present, PbTe cannot form

the two branches of a thermo-element. The p branch is therefore most often made of a TAGS type material (for tellurium-antimony-germanium-silver), which in turn makes it possible for the p branch to be most often made of a TAGS type material (for tellurium-antimony-germanium-silver), which in turn makes it possible to obtain merit factors greater than unity at 700 K only in type p [19]. Therefore, it is essential to develop a new material that can be used both p and n-type in this temperature range. It is industrially easier to use the same type of material for both branches (which would also make it possible to eliminate the highly toxic tellurium) [20].

D. High temperatures:

Alloys based on silicon and germanium exhibit good thermoelectric characteristics at high temperatures (above 1000 K) and are mainly used for the generation of electricity in the space domain [21], [22]. All the alloys of this type were used for the electricity supply of the Voyager probe.

I.3.2. New thermoelectric materials: (Intermetallic materials.)

A. Skutterudites:

Skuterrudites have a cubic structure (of the $CoAs_3$ type) composed of eight octahedra TX6 (with T = Co, Rh, Ir, and X = P, As, Sb), which are linked together by the vertices (figure I.3). The vibrations of the atom inserted into the vacant site will make it possible to reduce the thermal conductivity of the material by diffusion of the phonons and thus make it possible improving the thermoelectric performance of the material [23]. The smaller and heavier the inserted atom, the greater the amplitudes of vibration of the atom, which will be significant and will lead to a significant decrease in the lattice thermal conductivity. The ZT figure of merit reaches a value close to 1.4 for temperatures above 900°C [24] the major drawback of these compounds is their instability due to the sublimation of Sb at high temperatures.

The host atom was located in a green structure surrounded by yellow atoms (Bi, Sb, As, P, or N). Metal sites are shown in blue. The octahedral environment of these sites is shown in blue in the lower part of figure [25].
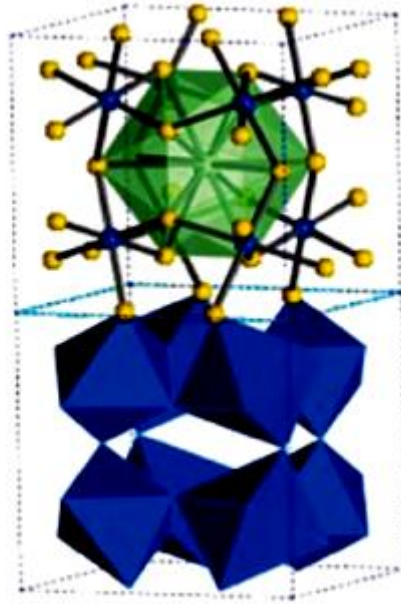
Figure I.3: Crystallographic structure of a skutterudite [25]

B. Clathrate:

Clathrates are periodic solids in which atoms (typically Si, Ge or Sn), linked together in the form of tetrahedrons, form a network of cages in which other types of atoms can be inserted [26] figure I.4 Indeed, these materials have a very low thermal conductivity, and a total or partial filling of the structure is possible. This was used to control the doping rate and power factor of the material.

The atomic lattice is shown in blue, whereas the host atoms are shown in purple orange, depending on the cage it occupies [25].

As a result, the chemistry of these compounds is also very rich, because it is possible to modulate the thermoelectric properties of these materials according to the nature of the filler atoms, and to work on atomic substitutions to optimize the electrical transport properties [27]. One of the highest ZT values observed for this type of material has been reported for $Ba_8Ga_{16}Ge_{30}$ (ZT = 1.35 at 900 K) [28]. However, controlling the stoichiometry of a compound is difficult, and can lead to the formation of secondary phases. In addition, clathrates exhibit insufficient corrosion resistance in air and melting points [29].

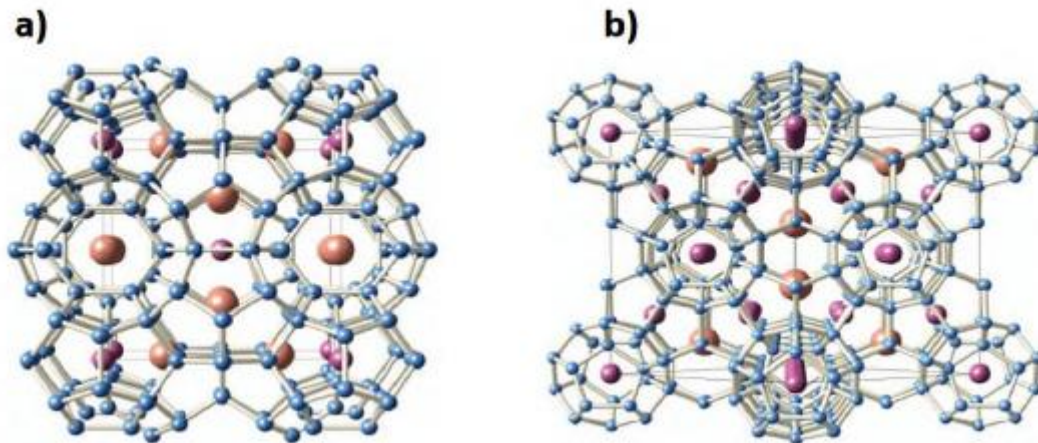**Figure I.4:** Crystallographic structures of type I (a) and type II (b) clathrates [26].

C. Zintl Phases:

Among the various "PGEC" materials currently being developed, phase-derived poly p-type ternary compounds are some of the most promising. These compounds have also been studied by NASA to be integrated at high temperatures (>900k), which is currently four times that of the alloys [30].

I.4. Applications in thermoelectricity:

Although the discovery of thermoelectric phenomena dates back to the beginning of the 19th century, Rayleigh only considered the idea of using these effects as a source of electrical or thermal energy in **1885** by Rayleigh **[31]**.

Until recently, a common application of this phenomenon was the use of thermocouples for temperature measurements. Thermoelectric devices, also called "modules," consist of an assembly of p- and n-type semiconductors electrically connected to each other in series and thermally connected in parallel, and are generally arranged between two ceramic plates. Thermoelectric devices, also called "modules," consist of an assembly of p- and n-type semiconductors electrically connected to each other in series and thermally connected in parallel, and are generally placed between two ceramic plates.

These devices are completely silent because their operation does not cause any vibration.

Until recently, these devices were used in niche sectors because of their high cost (production process and compounds used). In addition, the low performance of these systems limits their use in areas where there are no alternative energy sources (especially in the space sector).

Currently, it is easy to obtain thermoelectric devices, especially cooling systems (Peltier effect modules). Additionally, many projects are related to the development of new thermal generators for the production of electricity from waste heat (in particular, produced by heat engines).

I.4.1. Peltier modules:

The current performance of thermoelectric devices is well suited to their use in refrigeration (figure I.5), containers used for transporting organs.

CHAPTER I: THERMOELECTRIC MATERIALS

Commercially available Peltier effect modules are widely used for cooling electronic components and systems (over-clocked microprocessors (figure I.5), laser diodes, etc.) to limit component heating, thereby increasing their performance and lifespan. These thermoelectric devices are also used for cooling electronic systems where the generation of vibrations must be avoided. (self-directed infrared air-to-air missiles) **[32]**.

Manufacturers are currently working on using the Peltier effect to create air-conditioning systems. In the automotive sector, this particularly reliable technology would lead to the production of more efficient reversible air conditioning systems than those currently in use.

In addition, these thermoelectric systems are more compact and simpler to manufacture than the current systems. Finally, they did not use any refrigerant gas (which affects the greenhouse effect) **[33]**. Amerigon has been marketed since **1999** as a model of heated or cooled automobile seat based on the use of thermoelectric devices.

Other research groups are also working on integrating Peltier-effect micro-devices into textile fibers, or even manufacturing thermoelectric textiles, to produce smart clothing capable of heating (or cooling) the skin **[34]**. This research is of great interest to the military to equip soldiers working in desert or polar environments with portable low-mass air-conditioning systems. These smart clothes could also be used by people working in areas of high temperature (e.g., firefighters, steelworkers, glass craftsmen).

Finally, the modules offer very precise temperature control (thermo-stabilization); therefore, they are used in certain measuring devices in which the temperature must be perfectly adjusted and stabilized (e.g., a polar meter) **[35]**.

Figure I.5: Microprocessor and camping cooler equipped with Peltier effect modules **[32].**

I.4.2. Thermo generators:

The best known thermo generators are radioisotope thermoelectric generators (RTG) **[36]**. These devices use natural radiation from the decomposition of radioactive elements ($238Pu$, $90Sr$ or $210Po$) as a heat source ($1000°C$). They have been developed for the power supply of equipment requiring stable and reliable energy, over several years, and without maintenance **[36].**

These generators are used, for example, for the power supply of systems placed in isolated or inaccessible environments (lighthouses and navigation beacons **[37]**, weather stations, or even, surprisingly, in certain pacemakers **[38]**).

The best-known use of RTGs is for space probes (Figure I.6) **[36]**. In this precise, the use of this type of generators is, when a probe is sent, the solar panels no longer receive enough solar radiation to power the instruments of the probe. RTG thermo generators have been proven to be highly reliable thermoelectric devices. Indeed, we can cite the example of the Voyager space probe, which was launched in **1967** and continues to transmit information from the confines of the solar system for more than 40 years after its launch.
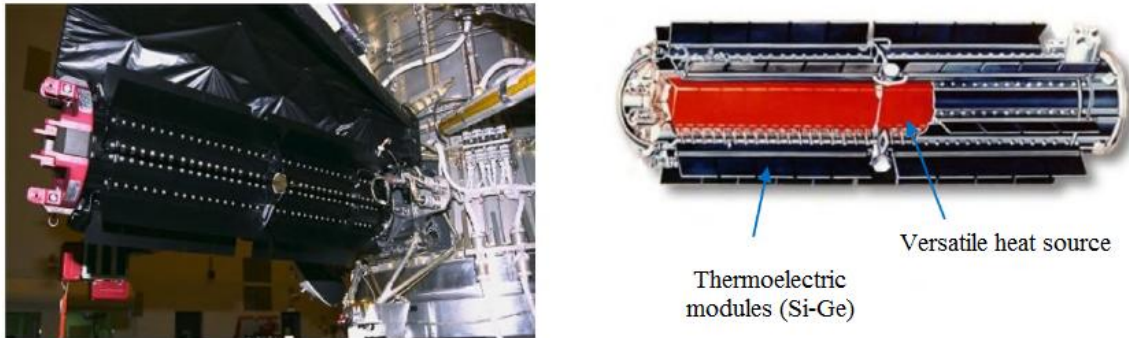
Figure I.6: Representation and description of the RTG **[36].**

Currently, the most promising use of thermo generators is the recycling of waste heat into electrical energy, particularly by using the enormous quantities of heat produced by industry and the automotive sector. Concerning the automobile, 70% of the energy produced by a thermal engine during the combustion of fuel is lost in the form of heat **[33] [39]**.

The use of thermo generators placed on the exhaust line would allow the transformation of this heat into electrical energy and could supply various electronic devices in the car (figure I.7). The energy produced by these thermo generators makes it possible to reduce the use of an alternator, leading to a reduction in fuel consumption.
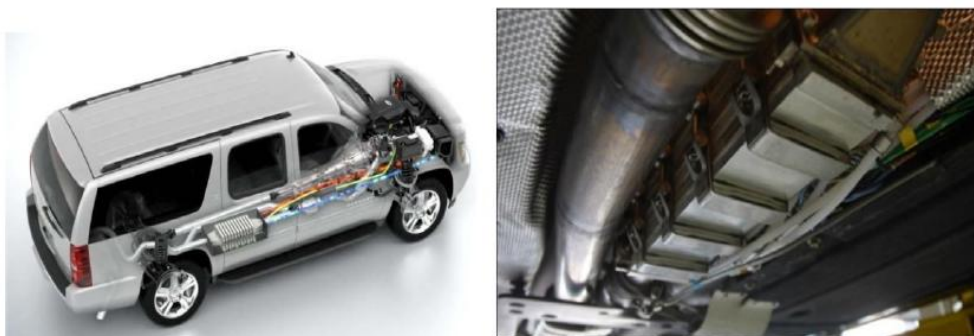

Figure I.7: Representations of thermoelectric generators fitted to vehicle prototypes **[39]**

14

Prototypes equipped with these devices (BMW, GM) are currently running, and tests have shown that at 125 km/h, the device generates electricity to dispense with an alternator, thus leading to a fuel saving of approximately 5 %. Thermo generators will, therefore reduce fuel consumption and greenhouse gas emissions.

Self-powered devices can be produced using the difference in heat between the human body and ambient air. The best-known example is the Seiko Thermal watch (figure I.8) **[40]**. The temperature gradient between the wrist and the ambient was 1 K. Modules implanted in the watch delivered a maximum of 22μW at 300mV and a voltage amplifier was used to increase the voltage to 1.5 V. Thus, it was possible to power the battery of the watch.

The use of thermo generators was also tested for the electrical supply of medical devices used for monitoring certain patients (figure I.8). This saves patients from frequent visits to medical centers associated with changing the battery fitted to the analysis device. The significantly increased autonomy of these medical devices allows remote monitoring of patients and an improvement in their comfort of life **[41].**

Figure.I.8: Watch and medical devices powered by thermoelectric devices **[44]**

Various studies have been conducted on the production of thermoelectric textiles. For the military, the possibility of equipping the soldiers of the future with "thermoelectric

clothing" would make it possible to supply all the tactical combat equipment worn by the soldiers (GPS, information transmission system, etc.). By using these textiles, a weight gain (up to 30%) is expected because the use of these thermogenerators would make it possible to dispense the batteries usually used for tactical equipment. In the civilian field, the use of these textiles would allow the creation of "smart clothes," allowing the recharging of mobile phones.

I.5. Conclusion:

In this chapter, various phenomena of electrical thermal conversion (Seebeck effect) and thermal electrical (Peltier effect) of energy are described.

This was followed by research by A.F. IOFFE in **1956** on thermoelectric semiconductors. The field of thermoelectricity went through a tough period, where no progress was reported until the **1990** when unexplained international interest gave thermoelectricity its renaissance with the discovery of new thermoelectric materials,increasing the figure of merit to values exceeding 1.

A number of application examples in the field of energy recovery or the generation of electricity from a heat source have been examined, as well as the use of thermoelectricity as a heat pump in certain applications.

We conclude from this chapter that we are only at the starting point in this field and that thermoelectricity will play a major role in the conversion of energy, and even eliminate certain conventional processes such as a heat pump using refrigerant gas.

CHAPTER II

PIEZOELECTRIC AND MAGNETOSTRICTIVE MATERIAL

II. 1.Introduction

The experimental discovery of piezoelectricity dates back to the year **1880**. It was the brothers Pierre and Jacques Curie, who were the first to observe that: certain crystals, when subjected to pressure in particular directions, positively and negatively charged certain portions of their surface. These charges are proportional to the pressure, and disappear when the pressure ceases. Therefore, piezoelectricity is a reversible phenomenon **[42]**. This first result corresponds to what is called the "direct" piezoelectric effect. The word piezoelectric comes from the Greek "piezo" meaning to squeeze or press. There is also a "reverse" piezoelectric effect sometimes called "reciprocal" or "inverse": when a piezoelectric crystal is polarized by an applied electric field, it deforms at a rate proportional to the applied electric field. This effect was predicted in **1877** by Lord Kelvin and experimentally verified by Pierre and Jacques Curie in **1881**. Subsequently, the formalism of piezoelectricity was developed by Duhem, Pickles, and Woldemar Voigt in **1894** **[42]**. The first industrial applications developed by Paul Langevin appeared during the First World War with ultrasonic waves for underwater measurement and detection. Since **1943**, technological progress has allowed the development of the first materials in the form of lead ceramics (PZT) with the basic formula $Pb(Zr_{1-x}Ti_x)O_3$. Currently PZT-type ceramics are used in many applications such as pulse generators, sensors, and actuators **[42]**. In this section, we present a general overview of the technology of materials, the phenomenon of piezoelectricity, and the properties of certain electrically polarized bodies under the action of mechanical constraints, and vice versa, when a field is applied to them. These two effects were inseparable.

II.2 Piezoelectric materials

Piezoelectric materials can be grouped into three main classes **[43]**:

II.2.1.Crystals

Crystals, the best known of which is quartz SiO_2, have little interest in applications such as ultrasonic generators. Their main drawbacks are the high piezoelectric constants, as well as a too low electromechanical coupling coefficient.

II.2.2. Polymers

Polymers such as partially crystallized poly-vinylidene-difluoridene (PVDF) can be used to obtain smoother materials that are mechanically adapted to large deformations or underwater acoustics in reception. PVDF is the best-known representative, and polymer chains can be oriented when an electric field is applied **[43]**.

II.2.3. Piezoelectric ceramics

Piezoelectric ceramics quickly impose themselves owing to their high piezoelectric coefficients. The ceramic family includes many elements, including barium-titanates which are the ancestors of current ceramics, lead titanates, and or lead meta-niobates used for high-resolution imaging. The PZT family (lead, zirconate, titanate) which appeared in **1954 [43]**, now constitute the first major source of ferroelectrics with a perovskite structure. The general formula of a perovskite is ABO_3, where the valence of the A cations is between +1 and +3 and the valence of the B cations is between +3 and +6. In the case of cubic symmetry, the A cations are located at the vertices of the cube, the B cations are in the middle of the cube and the oxygen atoms are in the center of the faces. The perovskite structure is thus composed of a network of BO_6 octahedra linked together by vertices and surrounded by cations A, (Figure II.1).
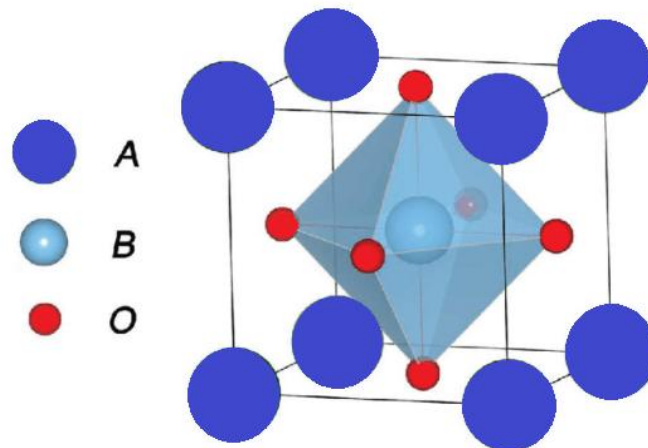
Figure II.1: Structure of perovskite of type ABO_3 **[43]**.

II.3. Piezoelectricity

Piezoelectricity is a property of certain materials (crystals, ceramics, polymers or composites) that can transforms electrical energy into mechanical energy.

The electric charge, which is a direct piezoelectric effect, is proportional to the imposed mechanical stress. The reciprocal effect, also called the inverse effect, causes the application of an external electric field to cause the mechanical deformation of the material. The piezoelectric effect can only be observed in certain non-conductive bodies that possess crystalline anisotropy. Thus, the displacement of the loads occurred in a privileged direction under tensile or compressive forces. This polarization axis results from the creation of dipoles at the crystalline scale by separation of the barycenter of the positive and negative charges under the effect of deformation **[42]**.

II.3.1. Direct effect

A distinction is made between direct and inverse piezoelectric effects. The direct effect is a phenomenon that results in the appearance of an electric field when the material is subjected to mechanical stress (F), as shown in Figure (II.2).
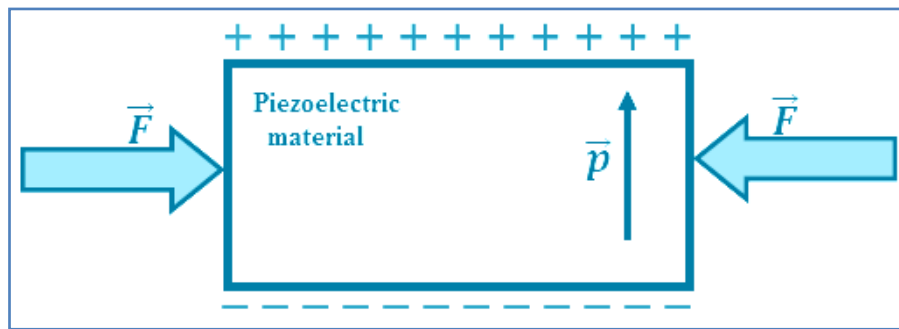
Figure II.2: Direct effect of a piezoelectric material **[42]**

II.3.2. Opposite effect

The piezoelectric effect is reversible. A piezoelectric material subjected to an electric field (E) undergoes deformation under the influence of internal forces. This deformation changes direction with the direction of the applied electric field, as shown in Figure (II.3).
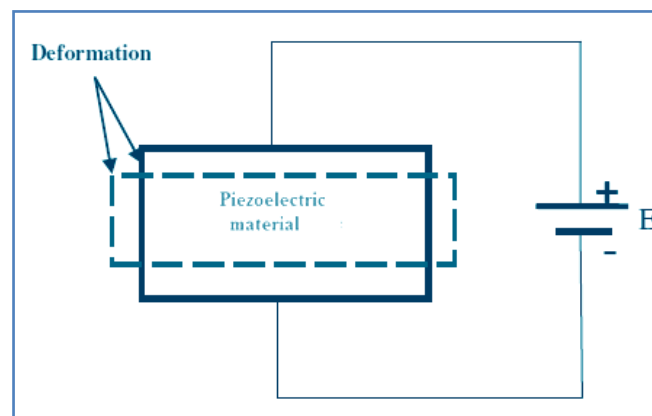
Figure II.3: Inverse effect of a piezoelectric material **[42]**

Only the non-centrosymmetric material classes exhibited a piezoelectric effect. Indeed, in these materials and at the scale of the mesh, the barycenters of the positive and negative charges no longer coincide when they undergo an action coming from the outside: a mechanical force, as shown in Figure (II.4) **[43]**.

Therefore, the piezoelectric effect can easily be explained by the appearance of electric dipoles induced by these charges within the crystal lattice. In nature, the materials are divided into 32 classes. Among these 32 classes, only 21 are non-centrosymmetric,

and 20 are array piezoelectric (Table II.1). Among them, there are 10 materials whose polarization varies according to the temperature and are called pyroelectrics.

Ferroelectric materials, which are a subgroup of pyroelectrics, have various structures including perovskites and pyrochlores. Those with a perovskite structures have been the most studied in piezoelectricity. For example, barium titanite ($BaTiO_3$), the first ferroelectric material in the form a ceramic, was discovered in the mid-**1940** and which has interesting properties **[43]**.

Then there is Lead zircono-titanate (PZT) was discovered a few years later and has since been supplanted ($BaTiO_3$) because of its high piezoelectric performance and high Curie temperature **[43]**.
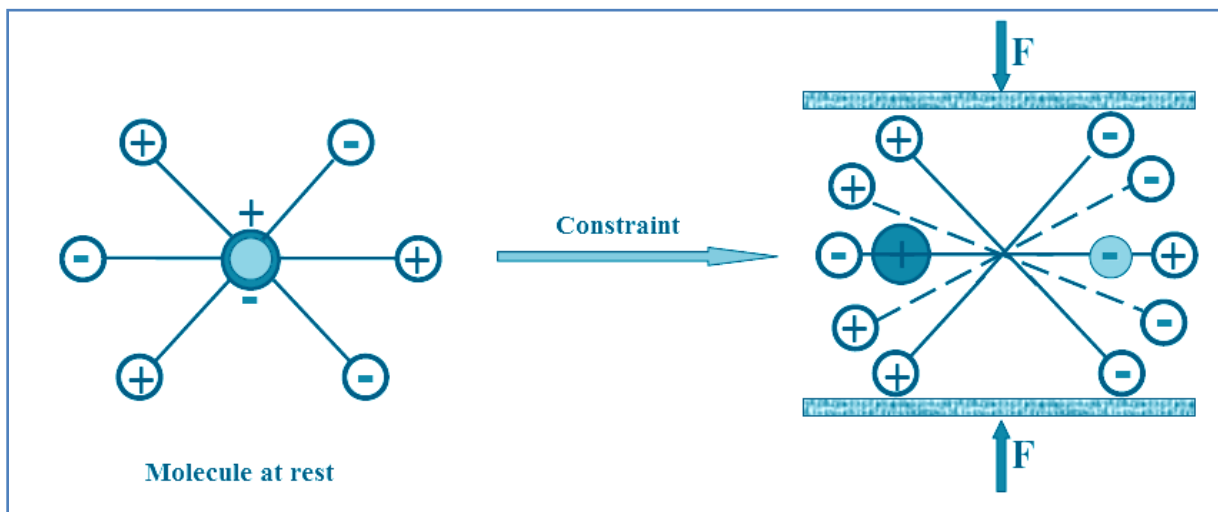
Figure II.4: Effect of mechanical action (stress) on a molecule with non-centrosymmetric (polar) symmetry **[43]**.

II.4. Ferro electricity

Ferro-electricity forms a subgroup of pyroelectricity, as shown in Table II.1. The polarization direction of the ferroelectric crystal varies depending on the external electric field. It can simply be reoriented or even reversed if the field is sufficiently strong **[43]**. Muller first used the term ferroelectric in 1935 to describe the hysteretic behavior of macroscopic electric polarization as a function of the applied electric field.

Ferroelectric materials do not exhibit any piezoelectric macroscopic properties prior to polarization. Once polarized, it becomes piezoelectric.

Table II.1: Crystalline classes of materials and the origin of the piezoelectric phenomenon

32 crystal classes				
11 centrosymmetric	21 Non-centrosymmetric			
11 non-piezoelectric	20 Piezoelectric			1 non-piezoelectric (cubic class 432)
	10 Pyroelectric : polar		10 non-pyroelectric : non polar	
	9 Ferroelectric	1 Non-Ferroelectric	10 Non-Ferroelectric	
	Example: BaTiO$_3$ PbTiO$_3$ KNbO$_3$	Example: Tourmaline	Example: Quartz	

II.4.1. Polarization

Ferroelectrics are materials whose polarization axes can be reoriented by subjecting them to a sufficiently strong electric field [43, 44].

- From a macroscopic point of view, the "unpolarized" ferroelectric material is organized into different domains of random polarizations, from which there is zero macroscopic polarization, as shown in Figure (II.4.a).

- The material was subjected to an electric field, as shown in Figure (II.4.b) tends to realign its different domains in the direction of the application of the field; the material is then macroscopically polarized (Ps polarization).

- This polarization effect is "remanent," i.e. when the electric field is removed, all the domains do not return to a state of random orientation and there is then a macroscopic state of remanent polarization (Pr) of the material, figure (II.4.c).
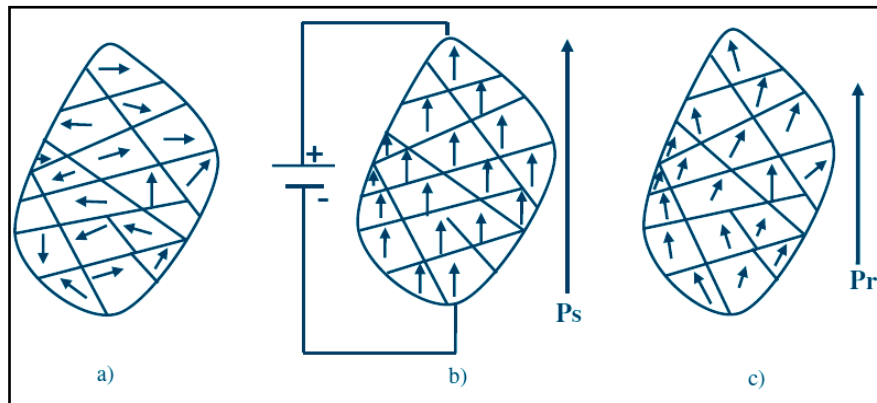

Figure II.4: Schematization of domains a) before polarization, b) during polarization, and c) after polarization **[42, 43]**.

II.5. Hysteresis cycle

The polarized ferroelectric material exhibited zero-field remanent polarization. The evolution of the polarization as a function of the field appears in the form of a hysteresis cycle, $P = f(E)$ (Figure II.5). The coercive field E_G is the electric field necessary to reorient the dipoles of a ferroelectric material.

Reman polarization P_r corresponds to zero-field polarization . Under high field values, we have a saturation polarization P_s **[44]**.

A ferroelectric material can be polarized if it is subjected to an electric field greater than the coercive field. Polarized ferroelectric materials exhibit piezoelectric properties.
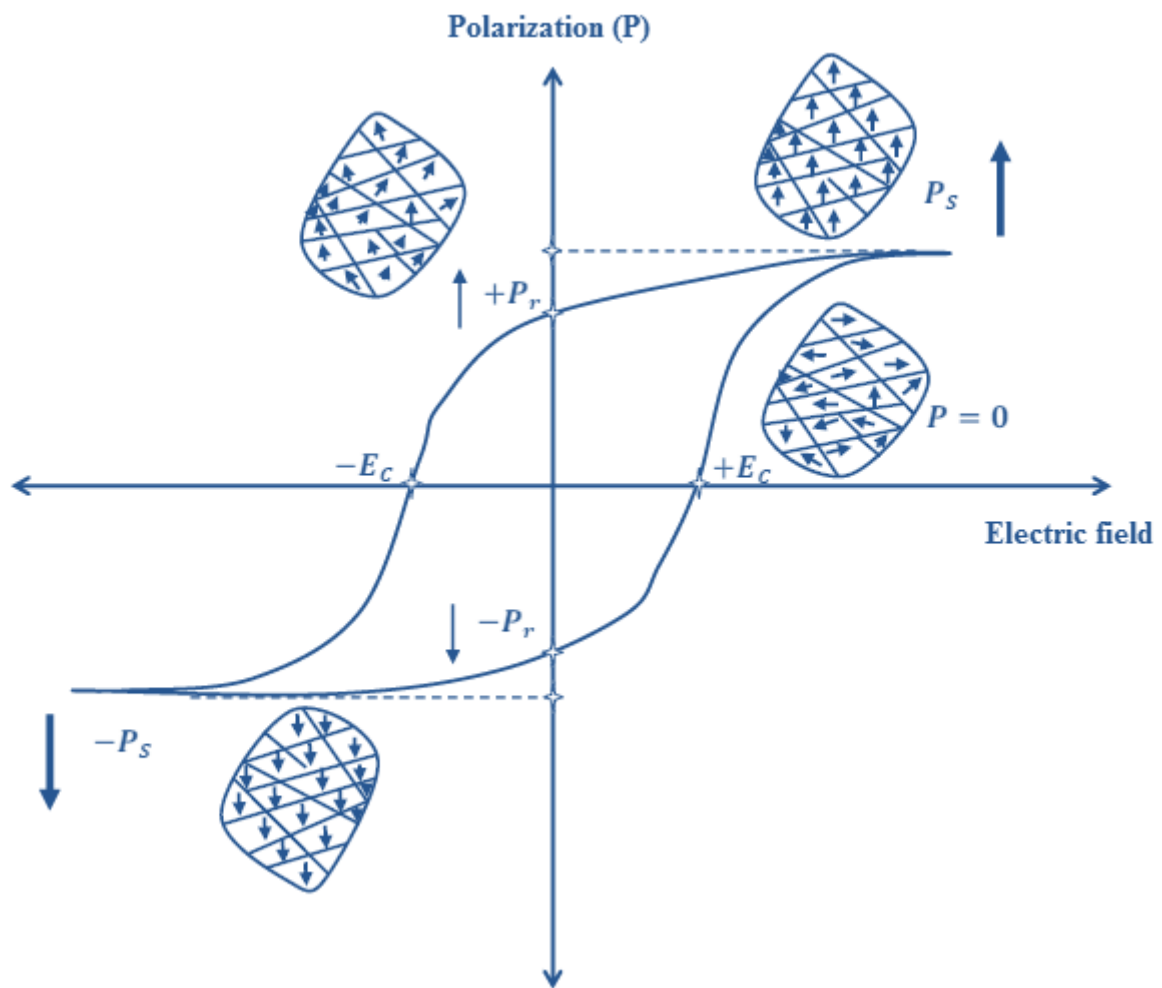
Figure II.5: Polarization hysteresis cycle of a ferroelectric material **[44]**.

II.5.1 Curie temperature and phase transitions

The phase transition of a ferroelectric material corresponds to a change in the crystalline structure, which generally occurs at a well-defined temperature and is accompanied by a modification in the orientation and/or amplitude of the electric polarization. The material changes from a ferroelectric to a para-electric state **[44]**.

The Curie point (Tc) is the temperature beyond which a ferroelectric material undergoes a structural phase transition to a state in which the spontaneous polarization of the lattice disappears. Beyond this temperature, the ferroelectric material was in a non-polar para-electric state. The polar-nonpolar transition corresponds to a phase transition **[44]**.

The crystal symmetry of the non-polar phase is always higher than that of the polar phase. At the Curie point, the relative dielectric permittivity is

$$\varepsilon_r = \frac{\varepsilon}{\varepsilon_0} \qquad \textbf{(II.1)}$$

reached the maximum value. Above this temperature, the ferroelectric material becomes para-electric, and ε_r follows the Curie-Weiss law :

$$\varepsilon_r = \frac{C}{T_\alpha - T_0} \qquad \textbf{(II.2)}$$

C: Curie constant;

T_0: Curie-Weiss temperature (°K);

T_α: absolute temperature (°K).

II.6. Choice of piezoelectric material

A comparison of the characteristic values of piezoelectric materials makes it possible to choose the most suitable material for the action to be used **[44]**. Table II.2 shows the piezoelectric characteristics of piezoelectric materials.

Table II.2: Physical constants of piezoelectric materials.

Parameters / material	Quartz SiO$_2$	*PVDF*	PZT
Density (g/cm^3)	2. 56	1.76	7.5
Dielectric constant e$_r$	4.5	12	200- 4000
Constant load $d_{33} \times 10^{-12}$ (C/N)	2	20	40-750
Constant voltage $g_{33} \times 10^{-33}$ (Vm/N)	50	190	15-40
Curie temperature (°C)	573	180	<350
Coupling coefficient K(%)	10	14	40-70

II.7. Applications of piezoelectric materials

Three main classes of piezoelectric material applications can be distinguished depending on whether the direct and/or inverse piezoelectric effect is involved (Table II.3) **[43]**.

Table II.3 : Applications of piezoelectric materials according to the effect used.

Applications based on the direct effect	Applications based on the inverse effect	Applications based on these two effects iclude
Microphone	Loud speaker	Diagnostic ultrasound transducer
Hydrophone	Buzzer	
Shock sensor	Sonar transducer	Ultrasonic NDT
Accelerometers	Inkjet printer	Proximity sensor
Strain/pressure sensor	Piezoelectric Pump	Piezoelectric transformers
		Gyroscope

II.8. Tensor equations for piezoelectricity:

The piezoelectric effect is a consequence of the coupling between the electrical and mechanical behaviors of a piezoelectric material. The anisotropy of piezoelectric properties of a solid involves the use of tensor expressions. First, it is necessary to define a system of axes to locate a piezoelectric material. By convention, the polarization axis was directed along the z-axis. An orthogonal reference trihedron oxyz is defined in accordance with the IEEE standard "IEEE Standard of Piezoelectricity" [Mee96]. The indices 1, 2, and 3 of Figure (II .6) correspond; to the directions of the axes, and Oz for the normal components, the indices 4, 5 and 6 to the planes; and for the tangential or shear components.
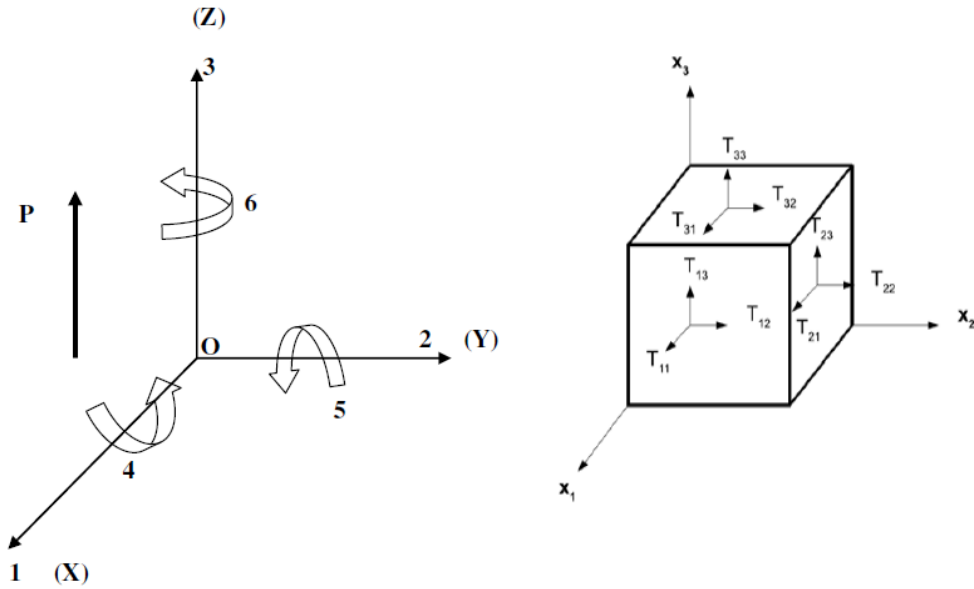
Figure II.6: Definition of conventional axes for a material **[42-44]**

When the phenomenon of pyroelectricity is negligible (i.e. the thermal effect is also negligible), the piezoelectric effect can be expressed by the eight fundamental equations linking the electrical quantities (electric field "E" and induction "D") to the mechanical quantities (stress "T" and strain "S") as indicated in Table (II.4).

Table II.4: Piezoelectricity equations

Independent variables	Mechanical quantities	Electrical quantities
(S, D) as a function of (E, T)	$S = s^E.T + d^t.E$	$D = d.T + \varepsilon^T.E$
(T, E) as a function of (D, S)	$T = c^D.S + h^t.D$	$E = -h.S + \beta^s.D$
(S, E) as a function of (D, T)	$S = s^D.T + g^t.D$	$E = -g.T + \beta^T.D$
(T, D) as a function of (E, S)	$T = c^t.S + e^t.E$	$D = e.T + \varepsilon^s.E$

Table (II.4) presents a glossary of mechanical, electrical and piezoelectric quantities and their meanings used to describe the systems of equations, which are defined below **[42]**, **[43]**, **[44]**.

28

With:

X^t Transpose of matrix X;

X^E Indicates that quantity X is considered at constant electric field;

X^D Indicates that quantity X is considered at constant electrical induction;

X^T Indicates that quantity X is considered at constant stress;

X^s Indicates that quantity X is considered at constant deformation.

Table (II.5): presents the electrical, mechanical and piezoelectric quantities.

Symbol	Meaning	Unity	Dimension
$\vec{D}$	Electric displacement or induction	C/m^2	(3×1)
$\vec{E}$	Electric field	V/m	
ε	Electrical permittivity	F/m	(3×3)
β	Impermittivity components	m/F	
S	Elastic compliance	---	(6×1)
T	the strain	N/m^2	
s	the compliance under short-circuit conditions	m^2/N	(6×6)
c	Stiffness or elastic constant	N/m^2	
d	Piezoelectric coupling coefficient for stress charge form	C/N	(3×6)
e	Piezoelectric coupling coefficient for stress charge form	C/m^2	
g	Piezoelectric coupling coefficient for stress voltage form	$V.m/N$	
h	Piezoelectric coupling coefficient for stress voltage form	V/m	

The piezoelectric coefficients (d,e,g, and h) were identical for the electrical and mechanical behaviors of the piezoelectric material. This implies that piezoelectricity requires an interaction between these two behaviors.

As a special case, if the material is non-piezoelectric (d=e=g=h=0), the electrical and mechanical behavior are decoupled, **[42]**, **[43]**, **[44]**.

II.9.Matériaux magnétostrictifs

II. 9.1.Introduction

The first studies on magnetostriction date back to the middle of the 19th century, when Joule (**1847**) studied the influence of magnetic fields on the dimensions of a steel bar. Kittel (**1949**) offers a thorough introduction and detailed definition. Magnetostriction is characteristic of ferromagnetic materials and alloys. It was subsequently analyzed extensively by Bozorth (**1951**), Lee (**1955**), and Kikuchi (**1968**) **[45, 46]**. Magnetostriction refers to the property possessed by ferromagnetic materials of deformation according to the orientation of their magnetization, for example, under the influence of a magnetic field. As in piezoelectricity, we distinguish the direct effects, where the application of a magnetic field (or the variation of this field) produces a modification of a mechanical parameter, and the inverse effects, where the variation of a parameter or a mechanical constant of a material produces a modification of its magnetization, regardless of whether it is initially immersed in a magnetic field.

II.9.2.Main magnetostriction phenomena

II.9.2.1. Joule effect (longitudinal)

This is the most significant magnetostrictive phenomenon. It relates to the lengthening or shortening Δl of a ferromagnetic rod of length l under the action of a magnetic field (Figure II.7). $\Delta l/l$ is not a linear function of the field and Δl is independent of the direction of the field in one direction **[48]**.
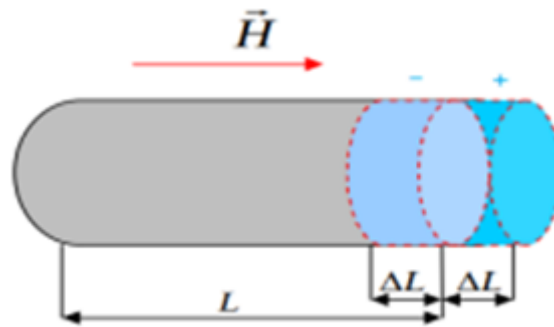
Figure II.7: longitudinal Joule effect **[48]**

II.9.2.2. Villari effect

The inverse longitudinal Joule effect is also known as Villari effect. When the natural length of bar of a ferromagnetic material is modified, the latter becomes magnetized (Figure II.8) **[48]**. If the bar is placed inside a solenoid, a transient current flows through the coil. This current corresponds to the variation in the magnetic flux associated with the variation in magnetization **[47]**. The strain Δl associated with a force differs from that predicted by classical Hooke's law. However, we can write:

$$F = ES_e\left(\frac{\Delta l}{l}\right)$$

With:

E: Young's modulus ;
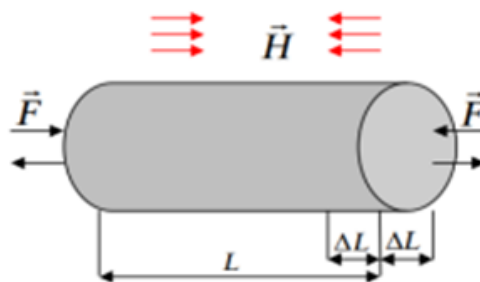
S_e : Cross section of the bar.

Figure II.8: Villari Effect **[48]**

II.9.2.3. Joule effect (transversal)

The transverse Joule effect was observed when the measurement direction was perpendicular to the magnetization (**Figure II.9**). The longitudinal and transverse Joule effects do not introduce any variation in volume if the material is isotropic or is composed of a disordered set of cubic crystals. However, this is not the case for elementary crystals with other symmetries **[48]**.
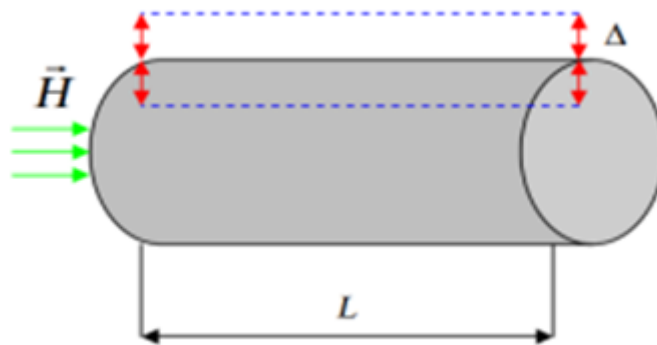

Figure II.9: Transversal Joule effect **[48]**

II.9.2.4. Wiedemann effect

This effect occurs when a bar or ferromagnetic magnet is subjected to a longitudinal field. If this bar is crossed by an axial current, the field associated with this current causes bar torsion (Figure II.10), which is known as the Wiedemann effect. The opposite effect produces a variation in the longitudinal magnetization and the appearance of circular magnetization in a long element magnetized axially and subjected to torque **[48]**.
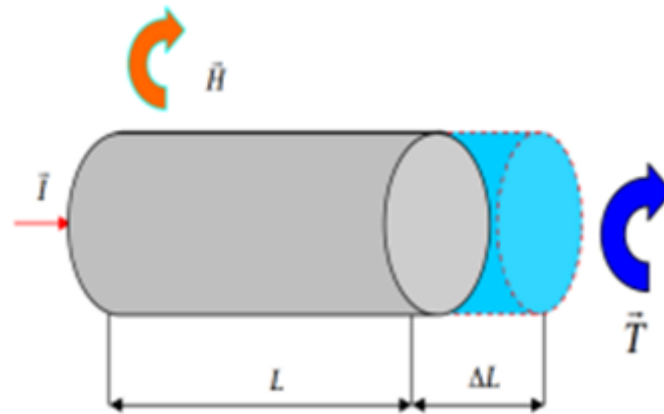
Figure II.10: Wiedemann Effect [48]

II.9.2.5. Effect of volume variations

Although the Joule effect occurs without volume change, there are magnetostrictive phenomena of volume change (ΔV) in ferromagnetic materials. There are several types of volume effects of different origins [48].

1- A spontaneous variation (without an applied field) of the volume was highlighted. A sample of a material then occupies a volume different from that which it would fill if it were not magnetic (Figure II.11). This volume variation is very large and positive for iron-nickel alloys at about 36% nickel ($\Delta V/V$ can reach in these alloys $1.9.10^{-2}$ At 0 K). Moreover, it decreases when the temperature increases and contributes by a term $\Delta V/(3V)$ to the partial compensation of the classical linear thermal expansion [48].

2- A spontaneous volume variation exists for other magnetic materials, but it is smaller. For example, it is equal in value to $-1.2.10^{-3}$ for nickel metal and $-2.7.10^{-3}$ for iron at room temperature. Volume variation was observed at a low field [48].
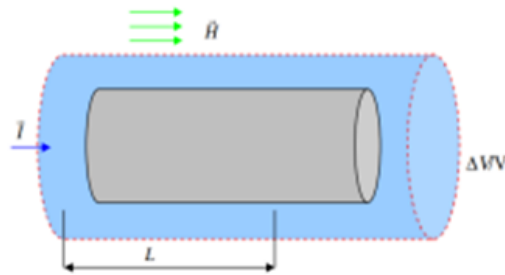
Figure II.11: Volume variation effect **[48]**

II.9.2.6.Bending effect:

Under the action of a longitudinal magnetic field, a bar embedded at one end undergoes a curvature, as if it were working in bending. This effect results in the transverse displacement of the entire free end of the bar under the action of a magnetic field (Figure II.12) **[48]**.
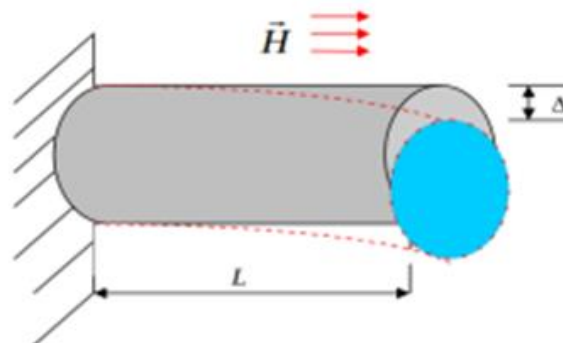

Figure II.12: Bending effect **[48]**

II.9.2.6.Effect of the Young modulus variability or δE effect:

When stress is applied to a ferromagnetic material, this causes a variation in magnetization which introduces deformation in addition to the deformation created by elasticity. This phenomenon corresponds to a modification of the elastic constants of the material, and therefore of its Young's modulus E (Figure II.13). The E-modulus is always reduced regardless of the sign of the magnetostriction coefficient λ_s of soft ferromagnetic materials that exhibit alignment of magnetic moments for very low stress at zero field, for saturating tensile **[48]**.
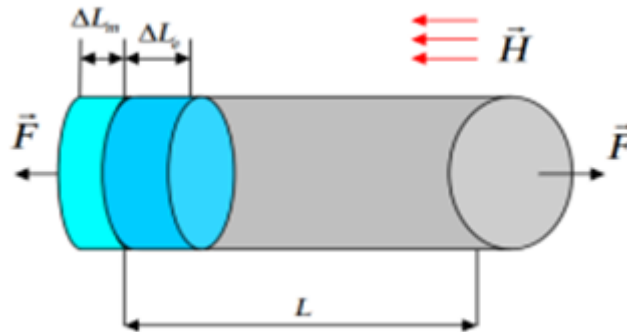
34

Figure II.13: Effect of the Young modulus variability **[48]**

II.10. Applications:

Magnetostriction is a loss component in power transformers, and is sought to minimize it. However, it also has positive applications in applications requiring low displacements with high force. However, the introduction of piezoelectric materials in the **1950** encroached on their domains because the coefficients of the known materials were low. Since **1970**, new materials, some of that exploit the magnetostrictive properties of rare earths elements, have revived the applications of magnetostriction **[48]**.

Direct and inverse magnetostrictive effects are exploited to build electromechanical actuators or sensors that convert electrical energy into mechanical energy and vice versa.

The main uses of magnetostriction are as follows:

- Emission of low-frequency sounds in an underwater environment (sonar).
- Ultrasound generation (medical or industrial applications).
- Production of linear motors (e.g., machine tools).
- Force and torque measurements.
- Active noise and vibration control simultaneously use the inverse effect for vibration measurement and the direct effect of corrective actions.

II.11. Conclusion

Piezoelectric materials are currently one of the best candidates for all applications requiring a massive ceramic, for example, for medical and biomedical applications or for the control of small displacements in mechanics to mobilize a quantity of fluid from the inlet to the outlet. The natural consequence of this type of development is a reduction in the dimensions and manufacturing costs with an acceptable yield. However, this field requires in-depth research into its materials and applications.

This chapter aims to recall the different notions of magnetostriction phenomena and present the necessary bases for understanding the physical mechanisms of magnetization of ferromagnetic materials. The performance of the magnetoelastic phenomenon is briefly discussed, where the essential elements concerning the general aspect and interest in magnetostriction are given.

Chapter III

Semiconductor

CHAPTER III: SEMICONDUCTOR

III. Introduction

Research on semiconductor materials began at the beginning of the 19th century. Many semiconductors have been studied over the past few years. Among the most famous, we find silicon (Si) and germanium (Ge) are found in column IV of the periodic table **[49]**. These two semiconductors are composed of identical atoms, others, such as gallium arsenide GaAs (III-V), are composed of atoms of different elements: Ga (III) and As (V). The composition of semiconductors makes it possible to determine electrical and optical properties of pure semiconductors. Before the invention of the bipolar transistor in **1947**, semiconductors were present in only two electronic devices; photodiodes and rectifiers. In the **1950s**, germanium (Ge) was used the most. However, they cannot be used in applications requiring low current consumption and/or high temperatures . Silicon, which is less expensive and allows low consumption applications, has been widely used since **1960**.

III.1. Energy Bands

Consider an isolated Si atom, the energy levels of its electrons are discrete (see the Bohr model for hydrogen) **[50]**. When an identical atom is brought closer to the latter, the discrete energy levels of its electrons are split into two under the reciprocal interaction of the two atoms **[50]**. More generally, when approaching N atoms, the energy levels split into N levels. These N levels are very close to each other and if the value of N is large, as is the case for a crystal, they form a continuous energy band. The notion of closeness of atoms is given by the inter-atomic distance d. Now, consider silicon (Si) atoms arranged at the nodes of a periodic lattice, but with a very large lattice in such a way that the atoms can be considered as isolated. The two highest energy levels were identified as E_1 and E_2. Bringing the atoms together homothetically, the electronic energy states split and form two continuous bands: conduction band (B_C) and valence band (B_V). Figure 1 shows the formation of these bands as a function of interatomic distance.
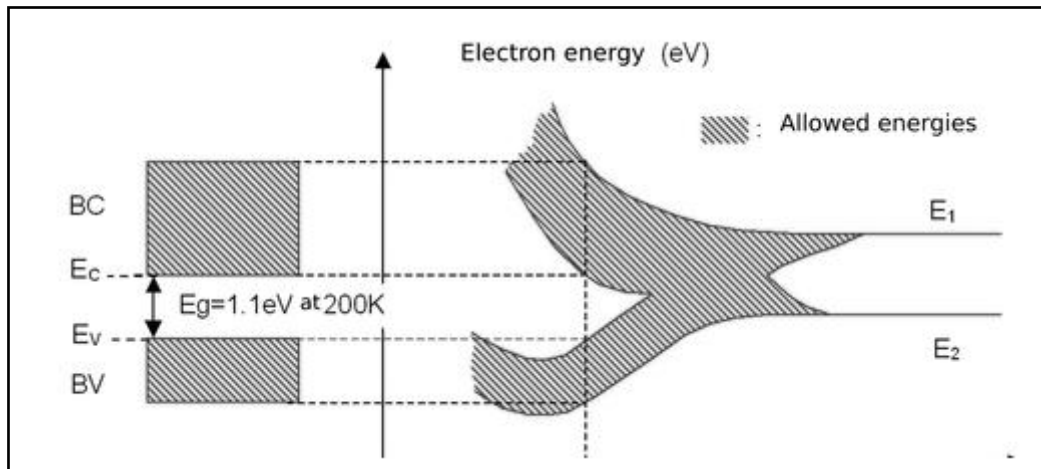
Figure III.1: Formation of energy bands for electrons in a silicon crystal with diamond-type lattice structure **[50]**

For the electrons of a crystal of silicon (d_0=2.35 Å), it can be seen that there are two continuous bands of energy (B_C and B_V) and that these bands are separated by a forbidden band because of energy inaccessible to electrons. This forbidden region is called "gap" and its width Eg is characteristic of the material. Note that the energy at the bottom of the conduction band is denoted as E_C and that at the top of the valence band is denoted as E_V; therefore, we have the equality $Eg=E_C-E_V$. Let us specify that the continuous bands of energy B_C and B_V are only a representation of the energies accessible by the electrons, this in no way presages the effective occupation of these bands by the latter **[50]**.

III.2. Insulator, semiconductor, conductor:

Solid materials can be classified into three groups: insulators, semiconductors, and conductors. We considered as insulators materials with conductivity $\sigma < 10^{-8}$ S /cm (diamond 10^{-14} S/cm), as semiconductors with conductivity 10^{-8} S /cm $< \sigma < 10^3$ S /cm (silicon 10^{-5} S/cm to 10^3 S/cm) and as conductors materials such as 10^3 S /cm $<\sigma$ (silver 10^6 S/cm). The electrical properties of a material are a function of the electronic populations of the different permitted bands. Electrical conduction results from the movement of electrons within each band. Under the action of an electric field

applied to the material, the electron acquires kinetic energy in the direction opposite to that of the electric field. Considering an empty energy band, it is obvious from the fact that it does not contain electrons and does not participate in the formation of an electric current. The same was true for the full band. Indeed, an electron can move only if there is a free place (hole) in its energy band. Thus, a material with empty or full energy bands is considered an insulator. Such a configuration is obtained for gap energies greater than ~ 9 eV because for such energies, thermal agitation at 300 K cannot cause electrons to pass from the valence band to the conduction band by breaking electronic bonds. Thus, the energy bands are either empty or full **[50]**.
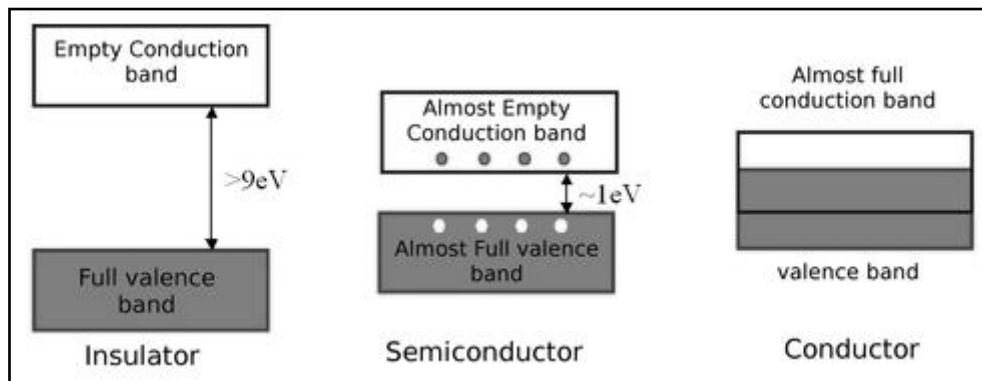
Figure III.2: Representation of energy bands **[50]**

A semiconductor is an insulator that operates at a temperature of 0 K. However, this type of material has a lower energy gap than the insulator (~ 1 eV) owing to thermal agitation (T= 300 K), a conduction band slightly populated by electrons and a valence band slightly depopulated. Knowing that the conduction is proportional to the number of electrons for an almost empty energy band and that it is proportional to the number of holes for an almost full band, we deduce that the conduction of a semiconductor can be qualified as "bad." For a conductor, the interpenetration of the valence and conduction bands implies that there is no energy gap between them. The conduction band is then partially full (even at low temperatures) and thus the conduction of the material is "high." **[50]**

III.3 Intrinsic semiconductors

An intrinsic semiconductor is an undoped semiconductor, that is, it contains few impurities (foreign atoms) in comparison with the number of holes and electrons generated thermally. To better understand the behavior of semiconductors, we need to study the populations of electrons and holes in each of the conduction and valence bands in more detail. In addition, we will perform an electronic balance of intrinsic semiconductors. To do this, we introduce the notion of the energy density, of states N(E). This quantity, which is dependent on the electronic energy E, corresponds to the space available for the electrons in the conduction band $N_c(E)$ and to the space available for the holes in the valence band $N_v(E)$. For energies close to the extrema of these two bands, the layout was parabolic.

$$N_c(E) = \frac{1}{2\pi^2} \left(\frac{2m_c}{\hbar^2}\right)^{\frac{3}{2}} \sqrt{E - E_c} \qquad\qquad \textbf{(III.1)}$$

$$N_v(E) = \frac{1}{2\pi^2} \left(\frac{2m_v}{\hbar^2}\right)^{\frac{3}{2}} \sqrt{E_v - E} \qquad [cm^{-3}/eV] \qquad \textbf{(III.2)}$$

Where $\hbar$= h/2 is the normalized Planck constant (h= 6.626.10^{-34} Js) and m_c (resp. m_v), effective mass of density of the states in the conduction band (resp. in the valence band). For direct gap semiconductors, m_c (resp. m_v), is the effective mass of an electron m_e (resp. of holes m_h) in the crystal. The concept of effective mass introduced in the preceding expressions makes it possible to treat the electrons (and holes) that are in the crystals of quasi-free particles, such as quasi-free particles. The semiconductor then becomes a gas of specific electrons and holes, owing to its effective mass, which is sometimes very different from that of a free particle. As an example for GaAs m_c/m_0= 0.066 with m_0= 0.911.10^{-30} kg the mass of the free electron **[50]**.

To obtain the effective number of electrons and holes in each band, the density of states is not sufficient, and it is also necessary to know the probability of the presence of an electron at an energy level E. This probability is given by the Fermi-Dirac function:

$$f(E) = \frac{1}{1+\exp\left[(E-E_F)/kT\right]} \tag{III.3}$$

Where k=1.38.10^{-23} JK^{-1} is the Boltzmann constant, T is the temperature, and E$_F$ is the Fermi energy, which is considered as the chemical potential in semiconductors. It goes without saying that the probability of occupation of an energy level E by a hole is 1-f(E) because the absence of an electron implies the presence of a hole and vice versa **[50]**.

The density of electrons n [cm^{-3}] in the conduction band is then obtained by summing over the entire energy range covered by this band, and the "space" available for electrons at energy E weighted by the probability to «find» an electron at the same energy level:

$$n = \int_{E_c}^{+\infty} N_c(E).f(E)dE \tag{III.4}$$

Similarly for the density of holes p [cm-^{3}] in the valence band:

$$P = \int_{-\infty}^{E_v} N_v(E).\left(1 - f(E)\right)dE \tag{III.5}$$

For a semiconductor whose Fermi level E$_F$ is distant from the extrema of more than 3kT, the Fermi function is simplified in an exponential form and we obtain for writing carrier densities:

$$n = N_c exp\left[-\frac{E_c-E_F}{KT}\right] \qquad N_c = \int_{E_c}^{+\infty} N_c(E).exp\left[-\frac{E-E_c}{KT}\right]dE \tag{III.6}$$

<div align="center">with</div>

$$p = N_v exp\left[\frac{E_v-E_F}{KT}\right] \qquad N_v = \int_{-\infty}^{E_v} N_v(E).exp\left[\frac{E-E_v}{KT}\right]dE \tag{III.7}$$

Where N$_c$ and N$_v$ are the equivalent (or effective) densities of the states. These represent the number of useful states at temperature T, in the respective energy band. Note that the relationship given by the product of the carrier density is independent of the Fermi level. Therefore, this is valid for both intrinsic and extrinsic semiconductors

(see the next paragraph). Note that it is similar to the law of mass action, similar to that of the self-ionization equilibrium of water ($[H^+][OH^-]=K_e$) **[50]**.

$$np = n_i^2 \text{ with } n_i = \sqrt{N_c N_v} exp\left[-\frac{E_c-E_v}{2kT}\right] \quad \text{(III.8)}$$

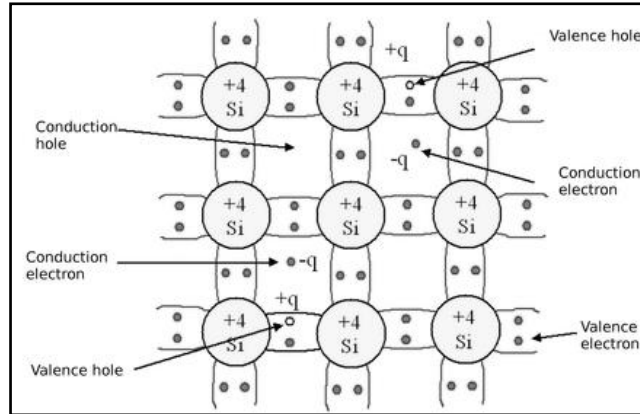Where n_i is the intrinsic carrier density (for silicon at 300 K, $n_i = 10^{10}$ cm^{-3}).

Figure III.3: Diagram showing the electronic bonds in an intrinsic semiconductor (Si) **[50].**

Figure 3 shows that for an intrinsic semiconductor (without impurities), each electron in the conduction band correspond to a hole in the valence band. From this observation, we deduce that the electron and hole densities are identical for this type of semiconductor **[50]**.

$$n = p = n_i \quad \text{(III.9)}$$

By replacing the carrier density with its respective expression, the previous equality allows us to define the Fermi level for an intrinsic semiconductor E_{Fi}. Knowing that at room temperature kT is much lower than the gap; this level is very close to the middle of the forbidden band:

$$E_{Fi} = \frac{E_c+E_v}{2} + \frac{KT}{2} ln\frac{N_v}{N_c} \cong \frac{E_c+E_v}{2} \quad \text{(III.10)}$$

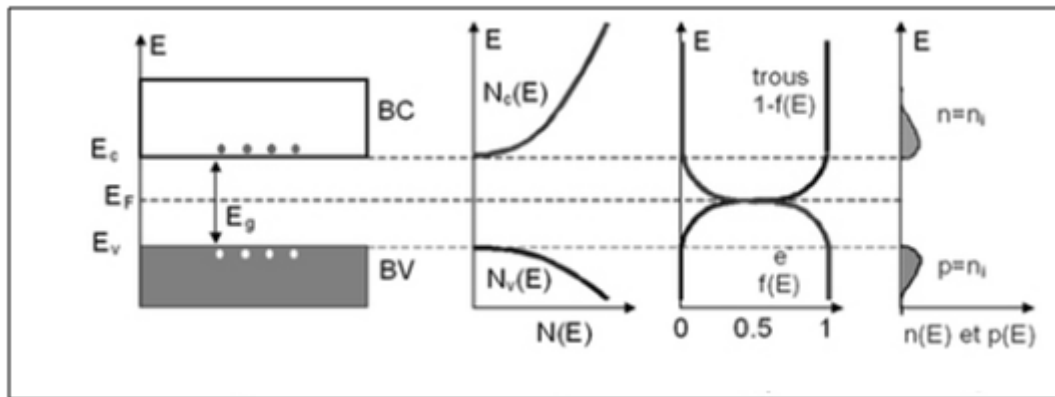Figure 4 graphically gives the electronic balance for an intrinsic semiconductor **[50]**.

Figure III.4: Intrinsic semiconductor **[50].**

III.4. Extrinsic semiconductors

An extrinsic semiconductor is an intrinsic semiconductor doped with specific impurities that provides electrical properties suitable for electronic (diodes, transistors, etc.) and optoelectronic (light emitters, receivers, etc.) applications **[50]**.

III.4.1. p-type semiconductors

A p-type semiconductor is an intrinsic semiconductor (e.g., silicon Si) into which acceptor-type impurities have been introduced (e.g., Bohr B). These impurities are called impurities because they accept an electron from the conduction band to form a bond with the semiconductor crystal **[50]**.

Figure 5 shows that a p-doped semiconductor has a lower density of electrons n and a higher hole density p than the same semiconductor in its intrinsic configuration. We then say that the electrons are the minority carriers and holes are the majority carriers **[50]**.
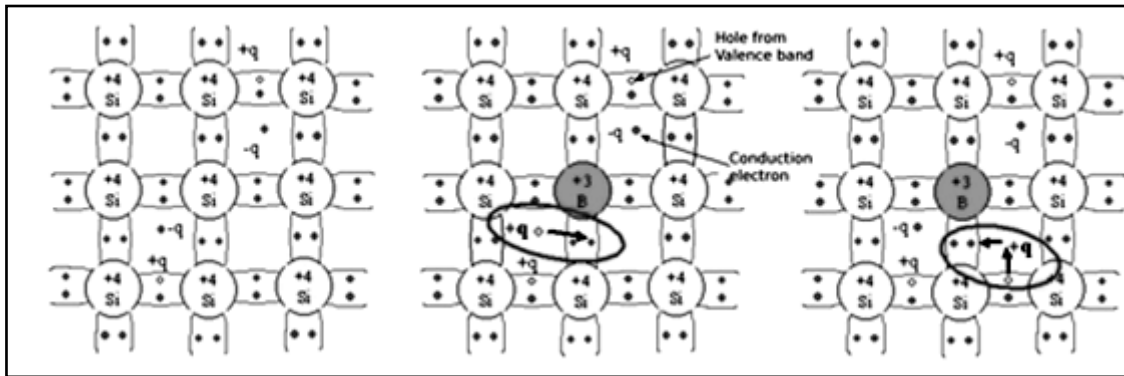
Figure III.5: schematic representation of a Si crystal doped with boron **[50]**.

For extrinsic semiconductors, the dopant density is always much higher than the intrinsic carrier density $N_A \gg n_i$. Therefore, in the case of the P-type, the hole density is therefore close to that of the N_A acceptor dopant. The relation is always verified, and we obtain the density of the carriers **[50]**:

$$n = \frac{n_i^2}{N_A} \tag{III.11}$$

$$p = N_A \tag{III.12}$$

The Fermi level for a P-type semiconductor or chemical potential is then:

$$E_{Fp} = E_v + KT ln \frac{N_v}{N_A} \tag{III.13}$$

Thus, the higher the density of acceptors, the closer the Fermi level approaches the valence band. At the limit of $N_A = N_v$ the Fermi level enters the valence band and the semiconductor is degenerate.

Figure 6 graphically shows the electronic balance of the P-doped semiconductor.
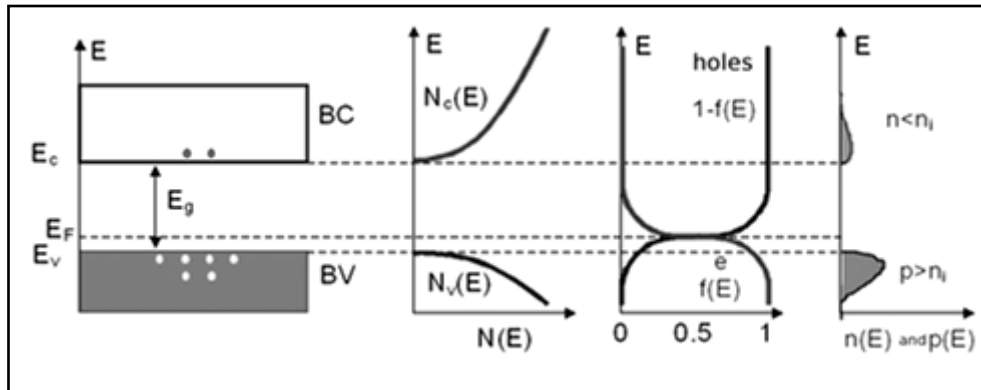
Figure III.6: P-type semiconductor **[50]**.

III.4.2. n-type semiconductors

An n-type semiconductor is an intrinsic semiconductor (e.g, silicon (Si)) into which donor-type impurities have been introduced (e.g, arsenic (As)). These impurities are so called because they donate an electron to the conduction band to make a bond with the semiconductor crystal **[50]**.
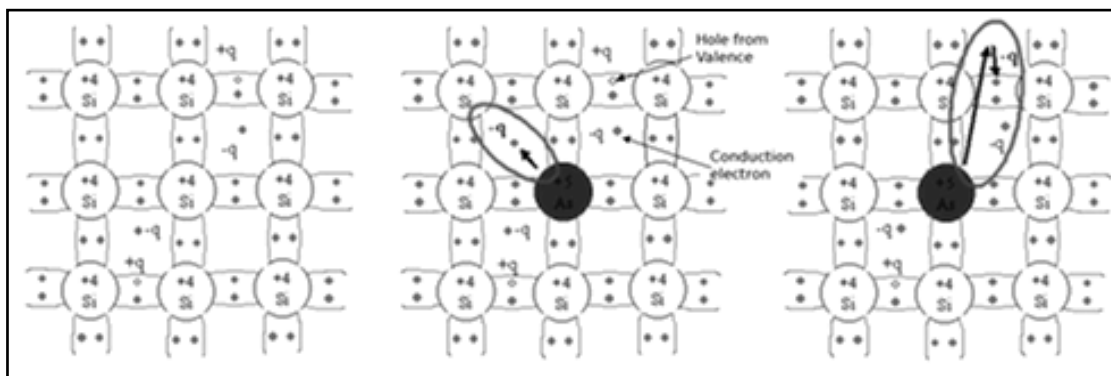

Figure III.7: Schematic representation of electronic bonds in a Silicon crystal doped with Arsenic As (n doping) **[50].**

Figure 7 show that an N-doped semiconductor has a higher n-electron density and lower p-hole density than the same semiconductor in its intrinsic configuration. We then say that the electrons are the majority carriers and the holes are the minority carriers.

By analogy with p-type semiconductors and denoting the N_D donor density, the carrier densities for an n-type semiconductor are:

$$N = N_D \tag{III.14}$$

$$p = \frac{N_i^2}{N_D} \tag{III.15}$$

The Fermi level for an n-type semiconductor is:

$$E_{Fn} = E_C - KTln\frac{N_C}{N_D} \tag{III.16}$$

Thus, the higher the acceptor density, the closer the Fermi level approaches the conduction band. At the limit of $N_D=N_C$ the Fermi level enters the conduction band, and the semiconductor is degenerate **[50]**.
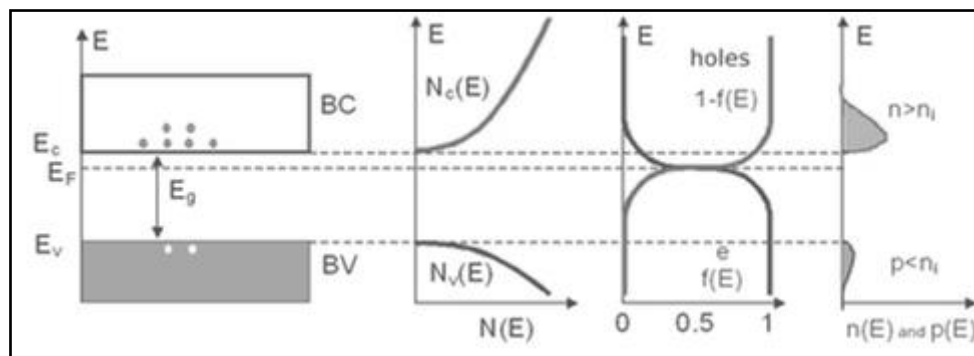

Figure III. 8: N-type semiconductor **[50]**.

III.5.Features

- Semiconductors are characterized by their dual functionality, energy efficiency, diverse applications, and low costs. The most notable characteristics of semiconductors are detailed below **[52]**.

- Your answer (conductive or insulator) may vary depending on the item's sensitivity to lighting, electric fields, and magnetic fields in the environment **[52]**.

- If the semiconductor is subjected to a low temperature, the electrons are held together in the valence band and therefore do not pose a free flow of electrons from the electric current [52].

- However, if the semiconductor is exposed to high temperatures, thermal vibration can affect the strength of the covalent bonds of the atoms of the element, which release electrons for the remaining electrical conduction [52].

- The conductivity of semiconductors varies depending on the proportion of impurities or doping elements inside an intrinsic semiconductor [52].

-For example, if 10 boron atoms are included in a million silicon atoms, this ratio increases the conductivity of the composites by a thousand times compared to the conductivity of pure silicon [52].

- The conductivity of semiconductors varies between 1 and 10^{-6} S.cm^{-1}, depending on the type of chemical element used [52].

- Extrinsic compounds or semiconductors can exhibit optical and electrical properties that are significantly superior to those of intrinsic semiconductors. An example is gallium arsenide (GaAs), which is primarily used in radio frequency applications and other optoelectronic applications [52].

Semiconductors are widely used as raw materials in the assembly of electronic elements that are a part of our daily lives, such as integrated circuits [52].

III.6. Application

Semiconductors are widely used as raw material in the assembly of electronic elements that are a part of our daily lives, such as integrated circuits [52].
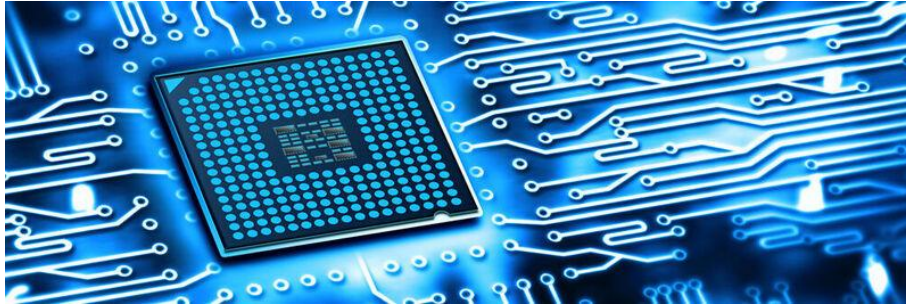
Figure III. 9: integrated circuit **[52]**

-One of the main elements of an integrated circuit is the transistor. These devices perform the function of providing an output signal (oscillatory, amplified or rectified) depending on a specific input signal **[52]**.

-Moreover, semiconductors are also the main material of diodes used in electronic circuits to allow the passage of electric current in only one direction **[52]**.
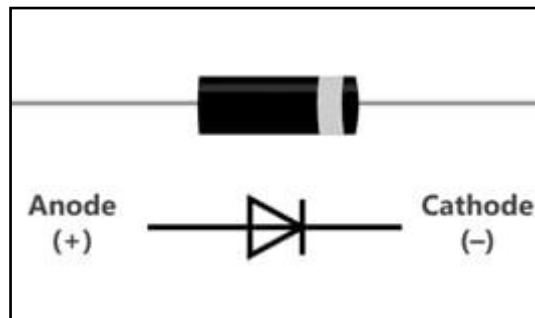

Figure III.9: Diodes[1]

[1.]A <u>diode</u> is a two-terminal electrical device. Diodes are made from semiconductors, most often silicon and sometimes germanium. There are various types of diodes (Zener, rectifier, schottky, transient voltage suppressor, thyristor, silicon controlled rectifier, and TRIAC) **[51]**.

- For diode design, extrinsic semiconductor p-type and n-type junctions form alternate Al carriers and electron donors, and a balancing mechanism between the two areas is activated **[52]**.

- Thus, the electrons and holes in the two areas intersect and complement each other if necessary. This can occur in two ways **[52]**.

- Transfer of electrons from the n-type zone to the p-zone. The n-type zone had a predominantly positive loading zone **[52]**.

- There is a passage of electrons carrying holes from the p-type zone to the n-type zone. The P-type zone has a negative charge **[52]**.

- Finally, an electric field is created that induces the flow of current in only one direction, that is, from zone n to zone p **[52]**.

- Additionally, using combinations of intrinsic and extrinsic semiconductors can produce devices that perform functions similar to those of a vacuum tube that holds its volume hundreds of times over **[52]**.

- This type of application applies to integrated circuits, such as for example microprocessor chips, which cover a considerable amount of electrical energy **[52]**.

- Semiconductors are present in electronic devices that we use in our daily lives, such as brown line equipment including televisions, video players, audio equipment, computers, and cell phones **[52]**.

III.6.1.Examples

- The most widely used semiconductor in the electronics industry is silicon (Si). This material is present in devices that make up integrated circuits, which are part of our daily lives **[52]**.

- Germanium and silicon alloys (SiGe) are used in high-speed integrated circuits for radars and amplifiers for electric instruments such as electric guitars **[52]**.

- Another example of a semiconductor is gallium arsenide (GaAs), which is widely used in signal amplifiers, especially for high-gain and low-noise signals **[52]**.

Chapter IV

Nanostructured Materials

IV. Introduction

The world market for nanoparticles was around 700 billion dollars for 2008 compared to 45.5 billion invested in **2004** and the "National Science Foundation" expects 1000 billion around **2010-2015**. Consequently, all industries are concerned with nanoparticles with specific magnetic, electrical, and optical properties **[53]**.

Many processes can produce these nanoparticles. We investigated gas-phase synthesis processes (condensation, pulsed laser ablation, spray pyrolysis, thermal plasma synthesis, etc.). Liquid-phase synthesis processes such as precipitation or reaction in a confined environment. Solid-phase synthesis processes involve precipitation of metals within a glass or polymer matrix **[53]**.

Grinding has emerged as one of the most widely used methods at an industrial scale. The ball mill technology has proven to be more useful for the production of nanoparticles. This constitutes a possible alternative to precipitation processes for natural or synthetic products that are not very soluble or insoluble in aqueous solutions **[53]**.

IV.1.Fields of application of nanostructured materials

In recent years, owing to their new physico-chemical properties, nanoscale structures have been intensively explored by researchers in different scientific fields (Nanobiology, Nanosystems, etc.). Here, we present an example of a field in which nanostructures play an important role **[54]**.

IV.1.1. Nanomagnetism

The dimensions of the crystalline domains significantly affect the magnetic behavior of the materials. Thus, the application of nanomaterials in the field of magnetism has enabled the development of new ranges of use in coercive and variable saturation fields, which are not achievable with conventional materials.

CHAPTER IV: NANOSTRUCTURED MATERIALS

IV.1.1. 1.Application of magnetic nanostructures to medicine

The interest in magnetic nanoparticles in medicine is owing to the possibility of their use as tools for remote control by a magnetic field, whose action under moderate conditions is negligible in biological media **[55]**. These particles can be super paramagnetic, or ferromagnetic.

IV.1.1.2. Application of magnetic nanostructures to magnetic recording

The use of magnetic nanostructures for recording and storing information is the most visible benefit of nanotechnology to the general public. Figure IV.1 gives, for example, the density of bits stored on hard disks according to the different stages of technological development **[67]**.

Nearly eight orders of magnitude in information density have been gained since IBM introduced the first hard drive in **1956**.

An electron is an electric charge carrier exploited in typical electronic components. In addition to its electric charge, it is associated with the mass of inertia and additional degrees of freedom, that is the spin. It is therefore possible to circulate spin-polarized electric currents in materials and to inject spins from one magnetic layer to another. This remarkable property of combining the electric charge and spin on the same object, the electron, has only recently been exploited under the name of spin electronics. To play on the spin polarization of the current, it is necessary to work with objects whose structure is controlled at the nanometric scale because the spin polarization diffuses over a typical length of the order of a few tens of nanometers. It is then possible to control the electrical properties using a magnetic field and vice versa. This produces spin valves (operating from the giant magneto-resistance effect or tunnel magneto-resistance) with ferromagnetic layers of a few nanometers. Spin-valve magnetic sensors are now integrated into all computer hard disk reading heads. An extraordinary property based on the inverse effect, that is, the possibility of controlling the magnetization state of a magnetic layer with a spin-polarized current, has recently been demonstrated. This property finds immediate application in M-RAM memory

allowing writing in a nanoscopic magnetic memory unit in the absence of an induced field **[67]**.
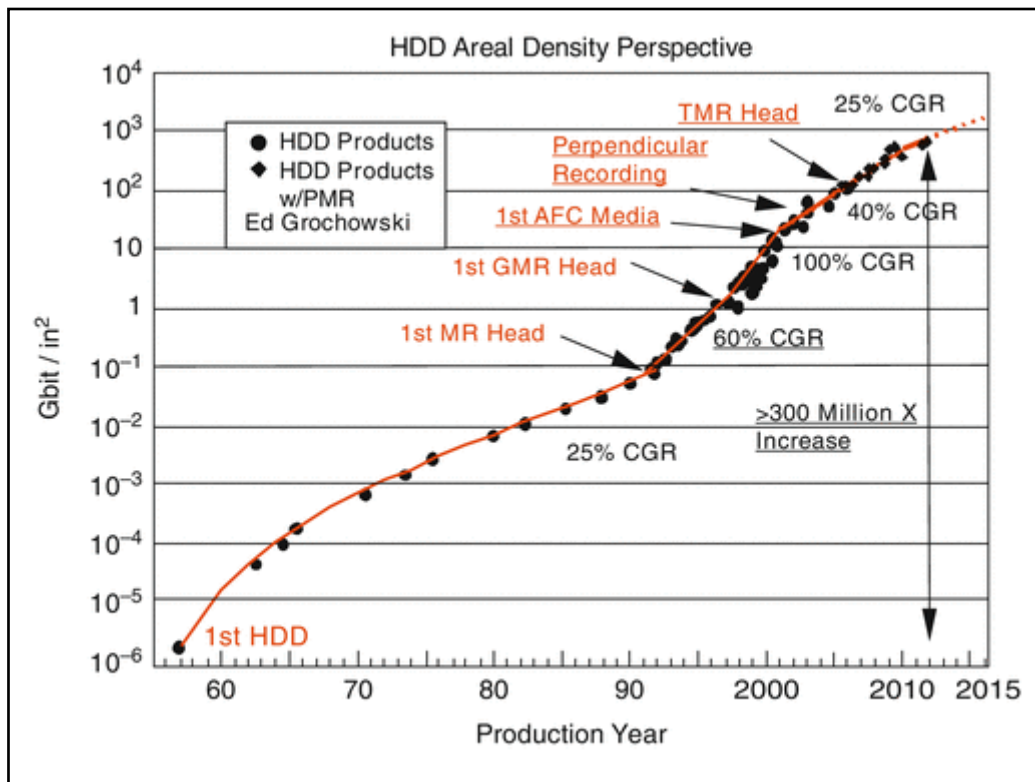

Figure IV.1: Compound growth rate (CGR) in areal recording density by year (reprinted with permission from **[67].**

IV.2. Structural characteristics

Nanostructured materials or nanomaterials are, by definition, solids in which at least one parameter varies on a nanometric scale: orientation of the crystal lattice, chemical composition or atomic density.

Thus, nonmaterials are defined as materials whose structures and physical properties are very diverse and are often characteristic of the production technique. Despite this diversity, all of these materials share three fundamental characteristics:

- Atomic domains confined to less than 100 nm in at least one dimension,

- A significant fraction of atoms is associated with an inter-facial environment.

- Interactions between various constituents.

IV.2.1. Classification

Nanomaterials can be classified into four families according to their form (see Figure.IV.2) [56]:

- Zero-dimensional materials consisting of nanometric grains are randomly dispersed or organized in a matrix. These are found, for example, in the colloidal crystals used in optics and magnetic fluids.
- One-dimensional materials which are in the form of nanowires or nanotubes;
- Two-dimensional materials are produced in the form of an ultrathin layer by the deposition of aggregates or atoms.
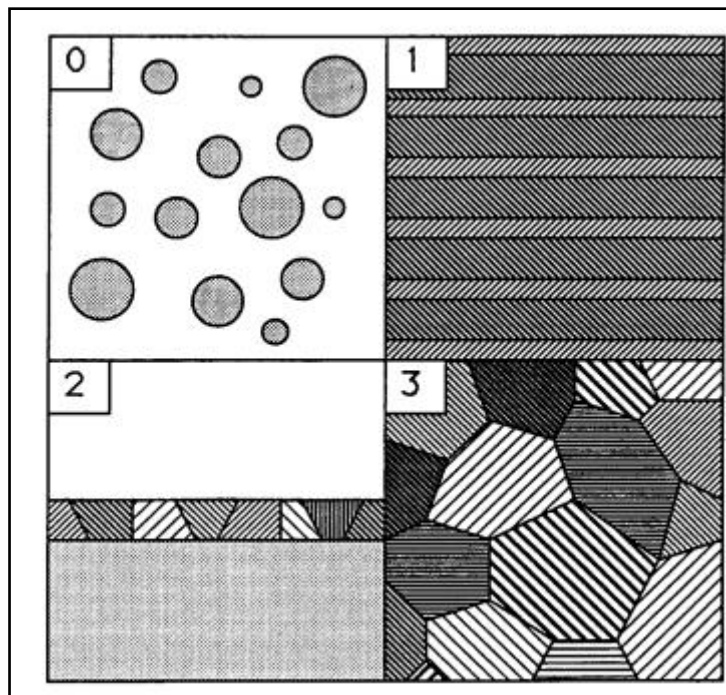- Three-dimensional materials have a compact form and are composed of single or polyphase grains.

Figure IV.2: Schematic of four types of nanostructured materials, classified according to integral modulation dimensionality: zero - clusters of any aspect ratio from 1 to ∞ ; one- multi-layers, two ultrafine-grained over-layers or buffed layers, and three- nanophase materials [56].

IV.2.2.1. Three-dimensional nanostructures

These are essentially nanophase materials made up of single or polyphase grains whose characteristic size is of the order of 1-100 nm. In general, they consist of two large families of atoms: those belonging to crystallized grains and those belonging to interfaces presenting a different distribution.

The development of such materials is based on several methods: soft chemistry, atom cluster consolidation, heat treatment of a metastable phase and mechanosynthesis. The nanocrystalline alloys obtained by partial devitrification of an amorphous phase consist of crystalline grains of nanometric dimension trapped in the residual amorphous matrix. Two families have been widely studied in recent years: the Finemet (FeCuNbBSi) and the Nanoperm (FeZrB) characterized by the appearance of FeSi grains of the centered cubic phase (cc) and Fe of the face-centered cubic phase (fcc). The nanometric-size scale of the grains gives these materials excellent magnetic properties (high magnetic permeability and strong magnetization at saturation).

Nanoscale siz of the grains gives these materials with excellent magnetic properties (high magnetic permeability and strong magnetization at saturation).

Two complementary approaches have been developed to synthesize nanostructured materials (see Figure IV.3):

In the first, so-called "bottom-up" approach, nanostructured materials are assembled from individual atoms or nanoscale blocks such as nanoparticles [57]. Among the technological methods for obtaining this type of nanostructuring, we can cite: compaction of the powder, chemical synthesis and all types of deposits can be cited.

The second approach is the top-down approach, which involves reducing the size of objects. Nanomaterials are produced by splitting larger materials. This approach is well known in the fields of microelectronics and microsystems.
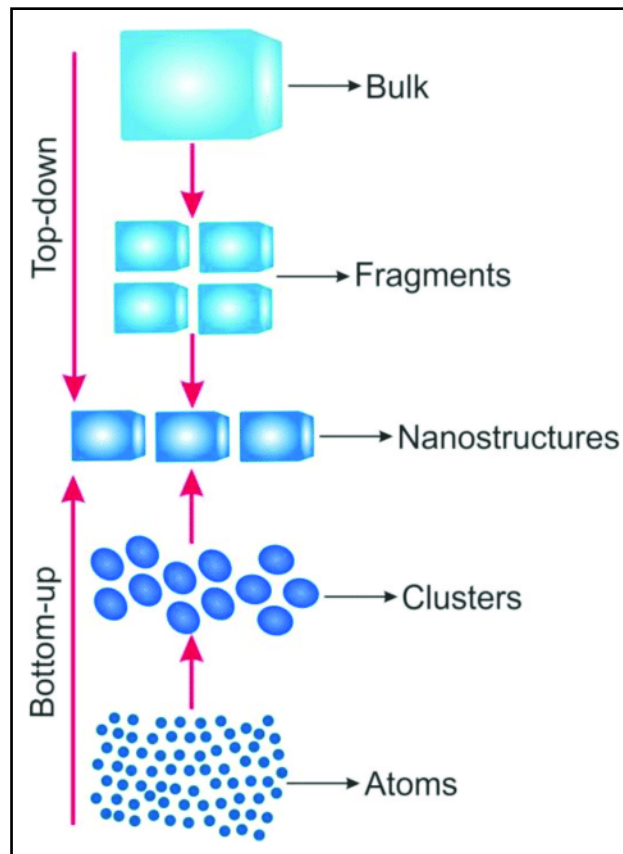
Figure IV.3: The schematic representation of top-down and bottom-up approaches for the fabrication of metal oxide nanostructures **[57]**.

The "top-down" approach requires precision technologies such as nanolithography **[57]**. This technique, which uses visible light, enables engraving of patterns of 100 nm. By replacing visible light with radiation of shorter wavelengths such as ultraviolet or X-rays, it is currently possible to engrave even smaller patterns on the order of 10-20 nm.

However, for magnetic nanostructures, the classification of nanomaterials proposed by Seigel in the early 90s was incomplete. According to Gleiter **[57]**, it does not distinguish between the dimensions of an object and its topology.

Therefore, the latter proposes a new classification that considers all of these criteria. A nano-object can also have one or two "non-nanometric" dimensions while presenting a

structure typical of nanomaterials. We then discuss the dimensions of orders 2, 1, or 0 depending on whether the object has one, two, or three nanometric dimensions.

The organization of nano-objects is also extremely important because it leads to collective behavior. We discuss the topology of orders 0, 1, 2, 3 depending on whether the objects are isolated, organized in chains, in a plane, or in a three-dimensional network (see figure IV.4).
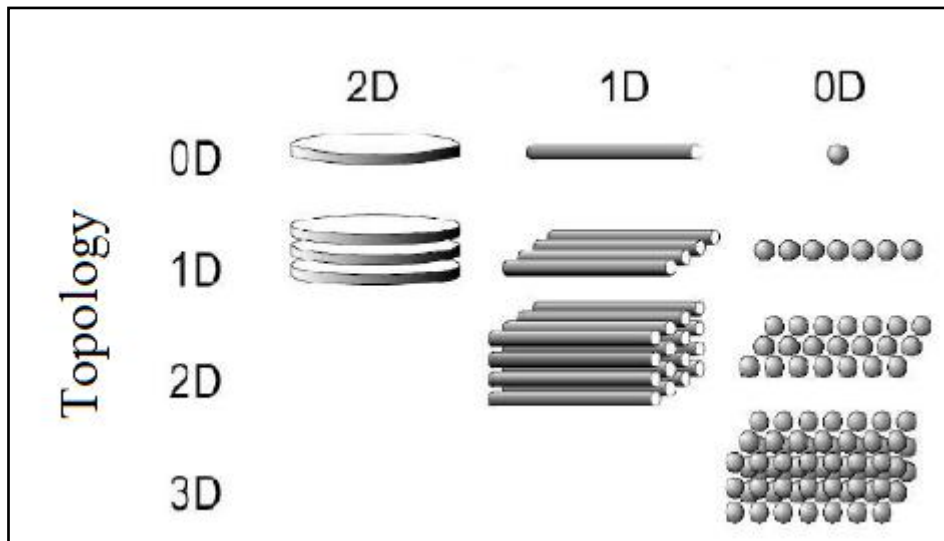

Figure IV.4: Classification of magnetic nanomaterial architectures according to the order of dimensionality of the nano-objects and topology **[57]**

IV.3. Origin of the difference in properties:

The origin of the difference in properties between bulk materials and nanomaterials is linked to the very large number of atoms belonging to the surfaces and interfaces in nanometric-sized materials. Indeed, when the size of a particle decreases, the number of particles per gram increases by a factor of 100 when the diameter of the particle changes from 100 to 1 nm **[58]**.

On the other hand, the reduction in the diameter of the particles leads to an increase in the proportion of atoms present on the surface (5% of the atoms of a 30 nm particle are on the surface against 20% for a 10 nm particle and 50% for a 3 nm particle). Figure IV.5 gives an example of the evolution of the percentage of atoms located on the surface as a function of the number of atoms constituting the nanoparticle. For some

nanomaterials obtained by "top-down" processes, there are atoms located on the surface, those belonging to the interfaces and which have an atomic distribution very different from that of the crystal grain **[58]**.

Figure VI.5: Inverse relationship between the total number of atoms in full shell clusters and the percentage of surface atoms in representation in hexagonal closepacked full-shell 'magic number' clusters **[58]**.

Nanostructured materials are essentially composed of two main parts; a crystallized phase and an interfacial phase with a disordered arrangement, commonly called the grain boundary **[59, 60]**. The decrease in grain size causes a large fraction of the atoms in these materials to localize at the interface. The volume fraction of atoms (Vg) in question is of the order Vg=3e/<d> where:

- e is the average effective thickness of the grain boundary.
- <d> is the average grain size.

For a thickness e ≈ 1 nm and a size of 10 nm, Vg is thus around 30%; the material then presents a simultaneous improvement of the physical and mechanical properties compared to those of the bulk material. Gleiter et al. synthesized nanostructured iron powders by the compaction of nanoparticles obtained by condensation in inert gas. The density measured on the discs was approximately 75% of that of the polycrystalline material. A study by Mössbauer spectrometry highlighted the presence of grain boundaries presenting a disordered structure, separating crystalline grains with a centered cubic phase (CC) **[61, 62]**.

A common characteristic of these systems is the strong influence of interfacial and surface zones on macroscopic properties. The surface effect or interface gives the material a two-phase characteristic. It is necessary to determine the chemical composition and structure of the surface or grain boundaries, including the number of nearby neighbors and density. In addition, the crystallographic orientation varies from one grain to another. Figure IV.6 presents a 3D nanostructure model composed of crystal grains separated by grain boundaries **[63]**.
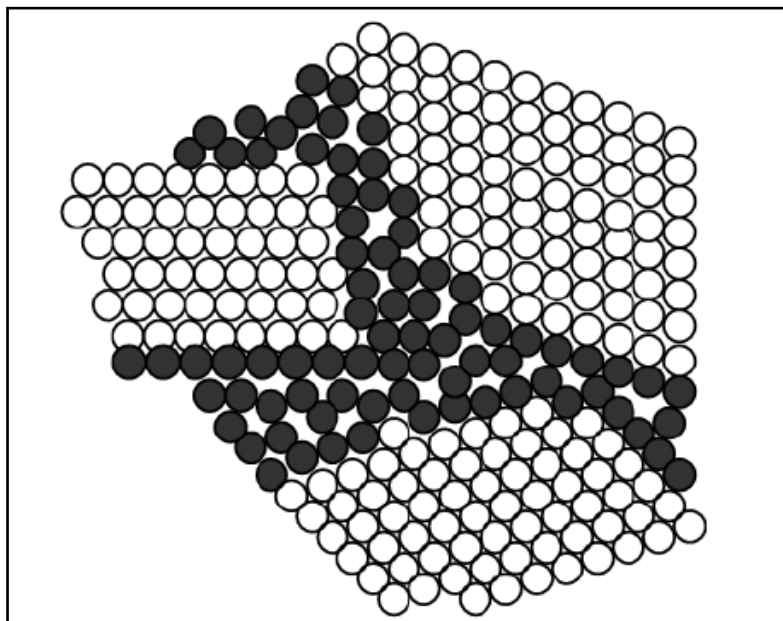
Figure.IV.6: Schematic representation of a 3D nanostructure, where crystallized grains (white) are linked by grain boundaries (black) with different topological and/or chemical order **[63]**.

IV.4. Methods for obtaining nanostructures

Several synthetic techniques have made it possible to obtain reproducible nanocrystalline materials by controlling their nanostructural parameters.These techniques can be classified into two categories **[63]**:

- One-step methods that directly produce solid materials with nanocrystalline structures, electrodeposition, recrystallization from the amorphous state, and plastic deformation.

- Two-step methods involve the synthesis of ultrafine powders followed by compaction to form a nanocrystalline material.

The inert gas condensation is a two-step process. However, this method has some drawbacks (embrittlement and corrosion), including the introduction of inert gases and other residual gases, such as oxygen and hydrogen, into the final material.

Another widely used method for the production of nanostructured powders is the mechanosynthesis technique; in this technique, the nanograins are obtained by decomposition of a powder composed of microcrystalline grains.

IV.5. Materials produced by high energy grinding

Two terms are commonly used in the Anglo-Saxon literature to refer to the high-energy reactive grinding process.

"Mechanical alloying" which is mechanosynthesis itself, a powerful tool allowing the production of metastable nanostructured powders from a mixture of elementary powders.

"Mechanical grinding" which is "direct" mechanosynthesis, mechanical grinding which consists of confining powders (of pure metal, intermetallic, or alloys) of stoichiometric composition to obtain a nanostructured material that is not necessarily homogeneous.

This technique has shown its ability to synthesize a variety of equilibrium or non-equilibrium alloy phases from parent alloys or elemental powders to produce oxide-dispersion alloys and iron-based alloys in the aerospace industry, a technique originally developed by Benjamin et al. **[64]**. The synthesized non-equilibrium phase can be described by a nanostructure, supersaturated solid solution, or metastable crystalline phase.

CHAPTER IV: NANOSTRUCTURED MATERIALS

Since the **1980s** the work of Suryanarana al. **[65]** and Koch et al. **[66]** demonstrated the potential of mechanosynthesis in the field of solid-state amorphization. There is profusion in the number of publications related to phase transitions induced by mechanosynthesis.

The development of new materials (amorphous, immiscible alloys, nanomaterials, high-temperature phases, etc.) on an industrial scale is because of their metastability, which requires synthesis techniques that limit the quantities produced. Mechanosynthesis does not have this drawback; for example, a laboratory-type grinder uses up to 10 g, and an industrial-type grinder can use up to one tonne.

Mechanosynthesis, which is easy to implement, should allow passage from the laboratory scale to the industrial scale, despite the low energy yield of this method. For these two reasons, metastability, and possible applications, mechanical synthesis has been the subject of numerous studies aimed at characterizing this process and understanding the mechanisms by which such varied materials can be produced. It also allows the preparation of alloys that cannot be obtained using conventional techniques.

CHAPTER IV: NANOSTRUCTURED MATERIALS

References

1. Thomas Johann Seebeck, Magnetische polarisation der metalle und erze durch temperatur-differenz. (W. Engelmann, 1895).

2. William Thomson, " Two Memoirs on the Dynamic Theory of Heat," Journal of Pure and Applied Mathematics", 209-252 (1852).

3. AI Ioffe, " Energy fundamentals of thermoelectric butters field conductors," Academy of Science of the USSR Moscow (1949).

4. Abram Fedorovich Ioffe, LS Stil'Bans, EK Iordanishvili, TS Stavitskaya, A Gelbtuch, and George Vineyard, "Semiconductor thermoelements and thermoelectric cooling," Physics Today 12 (5), 42 (1959).

5. Lyndon D Hicks and Mildred S Dresselhaus, "Effect of quantum-well structures on the thermoelectric figure of merit," Physical Review B 47 (19), 12727 (1993).

6. Lyndon D Hicks and Mildred S Dresselhaus, "Thermoelectric figure of merit of a one-dimensional conductor," Physical review B 47 (24), 16631 (1993).

7. Rama Venkatasubramanian, Edward Siivola, Thomas Colpitts, and Brooks O'quinn, "Thin-film thermoelectric devices with high room-temperature figures of merit," Nature 413 (6856), 597-602 (2001).

8. TC Harman, PJ Taylor, MP Walsh, and BE LaForge, "Quantum dot superlattice thermoelectric materials and devices," science 297 (5590), 2229-2232 (2002).

9. Kuei Fang Hsu, Sim Loo, Fu Guo, Wei Chen, Jeffrey S Dyck, Ctirad Uher, Tim Hogan, EK Polychroniadis, and Mercouri G Kanatzidis, "Cubic AgPb m SbTe2+ m: bulk thermoelectric materials with high figure of merit," Science 303 (5659), 818-821 (2004).

10. Akram I Boukai, Yuri Bunimovich, Jamil Tahir-Kheli, Jen-Kan Yu, William A Goddard Iii, and James R Heath, "Silicon nanowires as efficient thermoelectric materials," nature 451 (7175), 168-171 (2008).

11. JS Heron, T Fournier, N Mingo, and O Bourgeois, "Mesoscopic size effects on the thermal conductance of silicon nanowire," Nano letters 9 (5), 1861-1865 (2009).

12. Hyoungjoon Kim, Ilsoo Kim, Heon-jin Choi, and Woochul Kim, "Thermal conductivities of Si 1− x Ge x nanowires with different germanium concentrations and diameters," Applied Physics Letters 96 (23), 233106 (2010).

13. RD Abelson, "Space missions and applications, Thermoelectrics Handbook Macro to Nano", (C&C Press, Boca Raton, FL, 2006).

14. Claude GODART, Matériaux à effets thermoélectriques. (Ed. Techniques Ingénieur, 2009).

15. WM Yim and A Amith, "BiSb alloys for magneto-thermoelectric and thermomagnetic cooling," Solid-State Electronics 15 (10), 1141-1165 (1972).

16. Osamu Yamashita and Shoichi Tomiyoshi, "Effect of annealing on thermoelectric properties of bismuth telluride compounds," Japanese journal of applied physics 42 (2R), 492 (2003).

17. HJ Goldsmid, "Applications of Thermoelectric Refrigeration", in Thermoelectric Refrigeration (Springer, 1964), pp. 210-223.

18. ZH Dughaish, "Lead telluride as a thermoelectric material for thermoelectric power generation," Physica B: Condensed Matter 322 (1-2), 205-223 (2002).

19. JW Sharp, presented at the Proceedings ICT'03. 22nd International Conference on Thermoelectrics (IEEE Cat. No. 03TH8726), 2003 (unpublished).

20. Mohamed Amine Zoui and A BENATILLAH, "Study and realization of a thermoelectric cooling system powered by solar energy" Ahmed Draia-ADRAR University, 2017.

21. B Abeles, DS Beers, G Dr Cody, and JP Dismukes, "Thermal conductivity of Ge-Si alloys at high temperatures," Physical review 125 (1), 44 (1962).

22. Osamu Yamashita and Nobuhiro Sadatomi, "Thermoelectric properties of Si 1− x Ge x (x⩽ 0.10) with alloy and dopant segregations," Journal of Applied Physics 88 (1), 245-251 (2000).

23. GS Nolas, DT Morelli, and Terry M Tritt, "Skutterudites: A phonon-glass-electron crystal approach to advanced thermoelectric energy conversion applications," Annual Review of Materials Science 29 (1), 89-116 (1999).

24. BC Sales, DWRK Mandrus, and R KIFILLED Williams, "Filled skutterudite antimonides: a new class of thermoelectric materials," Science 272 (5266), 1325-1328 (1996).

25. George S Nolas, Joe Poon, and Mercouri Kanatzidis, "Recent developments in bulk thermoelectric materials," MRS bulletin 31 (3), 199-205 (2006).

26. John S Kasper, Paul Hagenmuller, Michel Pouchard, and Christian Cros, "Clathrate structure of silicon Na_8Si_{46} and Na x Si136 (x< 11)," Science 150 (3704), 1713-1714 (1965).

27. Ya Mudryk, Peter Rogl, C Paul, S Berger, Ernst Bauer, Gerfried Hilscher, C Godart, and H Noël, "Thermoelectricity of clathrate I Si and Ge phases," Journal of Physics: Condensed Matter 14 (34), 7991 (2002).

28. Ali Saramat, Göran Svensson, AEC Palmqvist, Christian Stiewe, Eckhard Müller, Dieter Platzek, SGK Williams, DM Rowe, JD Bryan, and GD Stucky, "Large thermoelectric figure of merit at high temperature in Czochralski-grown clathrate $Ba_8 Ga_{16} Ge_{30}$," Journal of Applied Physics 99 (2), 023708 (2006).

29. Julia V Zaikina, Kirill A Kovnir, Frank Haarmann, Walter Schnelle, Ulrich Burkhardt, Horst Borrmann, Ulrich Schwarz, Yuri Grin, and Andrei V Shevelkov, "The First Silicon-Based Cationic Clathrate III with High Thermal Stability: $Si_{172-x}P_xTey$ (x= 2y, y> 20)," Chemistry–A European Journal 14 (18), 5414-5422 (2008).

30. Shawna R Brown, Susan M Kauzlarich, Franck Gascoin, and G Jeffrey Snyder, "$Yb_{14}MnSb_{11}$: New high efficiency thermoelectric material for power generation," Chemistry of materials 18 (7), 1873-1877 (2006).

31. David Michael Rowe, Thermoelectrics handbook: macro to nano. (CRC press, 2018).

32. HJ Goldsmid, "Electronic Refrigeration. Pion Ltd", (London, 1986).

33. Jihui Yang and Francis R Stabler, "Automotive applications of thermoelectric materials," Journal of electronic materials 38 (7), 1245 (2009).

34. S Chatterjee, presented at the 6 th European Conference on Thermoelectrics (unpublished).

35. LB Ershova and GG Gromov, "Optimal thermoelectric cooling in laser diode sub-assemblies," RMT Ltd., Moscow (2006).

36. RC O'Brien, RM Ambrosi, NP Bannister, SD Howe, and Helen V Atkinson, "Safe radioisotope thermoelectric generators and heat sources for space applications," Journal of Nuclear Materials 377 (3), 506-521 (2008).

37. Eugene Levner, Igor Linkov, and Jean-Marie Proth, Strategic management of marine ecosystems. (Springer, 2005).

38. Christophe Chauvel, Thomas Lavergne, Ariel Cohen, Pierre Ducimetiere, JEAN YVES le HEUZEY, Jean Valty, and Louis Guize, "Radioisotopic pacemaker: Long-term clinical results," Pacing and Clinical Electrophysiology 18 (2), 286-292 (1995).

39. N Espinosa, M Lazard, L Aixala, and H Scherrer, "Modeling a thermoelectric generator applied to diesel automotive heat recovery," Journal of Electronic materials 39 (9), 1446-1455 (2010).

40. M Kishi, H Nemoto, T Hamao, M Yamamoto, S Sudou, M Mandai, and S Yamamoto, presented at the Eighteenth International Conference on Thermoelectrics. Proceedings, ICT'99 (Cat. No. 99TH8407), 1999 (unpublished).

41. Vladimir Leonov, Tom Torfs, Ruud JM Vullers, and Chris Van Hoof, "Hybrid thermoelectric–photovoltaic generators in wireless electroencephalography diadem and electrocardiography shirt," Journal of electronic materials 39 (9), 1674-1680 (2010).

42. Christophe Yamahata, "Magnetically Actuated Micropumps". Doctoral thesis, Federal Polytechnic School of Lausanne, 2005.

43. Zouhair Sadoune, " Modeling and simulation of Piezoelectric composite materials Case of SiO_2," (2013).

44. Arnaud Parent, "Contribution of new piezoelectric materials in the field of micro vibrating gyrometers". Doctoral thesis, Faculty of Sciences of Orsay – University of Paris-Sud, 2008.

45. Ahmed Younes Legmairi, " Use of neural networks to model the nonlinear behavior of magnetostrictive materials under the effect of mechanical stress," (2018).

46. Farid Hocini, Association of the command for the study by finite elements of the magneto-elastic and vibratory phenomena in the electrotechnical systems; Doctoral thesis specialty: electrical engineering, 2013.

47. Nicolas Galopin, "Modeling and characterization of active materials for the design of magneto-electric devices", Pierre and Marie Curie University, December 11, 2007.

48. Benabderrahmane Sofiane and Azrine Fawzi, "Design and modeling of an electromagnetic transducer based on magnetostrictive materials" Mouloud Mammeri University, 2016.

49. https://www.differencebetween.com/difference-between-silicon-and-vs-germanium

50. http://optique-ingenieur.org/en/courses/OPI_ang_M05_C02/co/Contenu.html

51. https://www.jameco.com/Jameco/workshop/Howitworks/different-types-of-diodes-and-how-they-work.html

52. https://www.thpanorama.com/blog/tecnologia/semiconductores-tipos-aplicaciones-y-ejemplos.html

53. Romain Gers, "Local analysis of the hydrodynamics of an agitated ball mill for the treatment of solid-liquid dispersions", doctoral thesis from the University of Toulouse, 2009.

54. Ahmed Haddad, "Non-destructive characterization of nanostructured materials produced by mechanosynthesis" University of Sciences and Technology Houari Boumediène (USTHB), 2011.

55. Karl Goser, Peter Glösekötter, Peter Glosekotter, and Jan Dienstuhl, Nanoelectronics and nanosystems: from transistors to molecular and quantum devices. (Springer Science & Business Media, 2004).

56. RW Siegel, "Nanostructured materials", in Advanced Topics in Materials Science and Engineering (Springer, 1993), pp. 273-288.

57. Vardan Galstyan, Manohar P Bhandari, Veronica Sberveglieri, Giorgio Sberveglieri, and Elisabetta Comini, "Metal oxide nanostructures in food applications: Quality control and packaging," Chemosensors 6 (2), 16 (2018).

58. Herbert Gleiter, "Nanostructured materials: basic concepts and microstructure," Acta materialia 48 (1), 1-29 (2000).

59. Günter Schmid, "Clusters and colloids: bridges between molecular and condensed material," Endeavour 14 (4), 172-178 (1990).

60. P Keblinski, SR Phillpot, D Wolf, and H Gleiter, "Thermodynamic criterion for the stability of amorphous intergranular films in covalent materials," Physical review letters 77 (14), 2965 (1996).

61. G Le Caër and P Delcroix, "Characterization of nanostructured materials by Mössbauer spectrometry," Nanostructured materials 7 (1-2), 127-135 (1996).

62. H-E Schaefer, R Würschum, R Birringer, and H Gleiter, "Structure of nanometer-sized polycrystalline iron investigated by positron lifetime spectroscopy," Physical Review B 38 (14), 9545 (1988).

63. Michel Wautelet, " Nanotechnology," (2009).

64. John S Benjamin, "Dispersion strengthened superalloys by mechanical alloying," Metallurgical transactions 1 (10), 2943-2951 (1970).

65. C. Suryanarayana, Mechanical alloying and milling, Progress in Materials Science V46, Issues 1-2, p1-184, 2001

66. Carl C Koch and JD Whittenberger, "Mechanical milling/alloying of intermetallics," Intermetallics 4 (5), 339-355 (1996).

67. Stefan Maat, Arley C Marley, Y Xu, DD Awschalom, and J Nitta, "Physics and design of hard disk drive magnetic recording read heads," Handbook of Spintronics; Xu, Y., Awschalom, DD, Nitta, J., Eds, 1-45 (2014).